Supporting Information

For the Manuscript Entitled

Size-selective Detection of Picric Acid by Fluorescent Palladium Macrocycles

Sushil Kumar,[†] Ram Kishan,[†] Pramod Kumar,[†] Sanya Pachisia and Rajeev Gupta*

Department of Chemistry, University of Delhi, Delhi 110007, India
E-mail: rgupta@chemistry.du.ac.in

[†]These authors contributed equally.

Content

1. Experimental Section

Materials. All reagents were obtained from the commercial sources and were used as received. Solvents were purified according to standard literature procedures. 3-(diphenylphosphino)aniline and 4-(diphenylphosphino)aniline were synthesised according to the procedure filed for the patent (201611008186). HPLC grade solvents were used for the UV-visible and fluorescence spectral studies.

2. Synthesis of Ligands

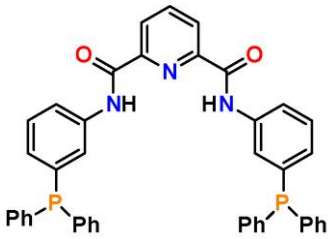

L1

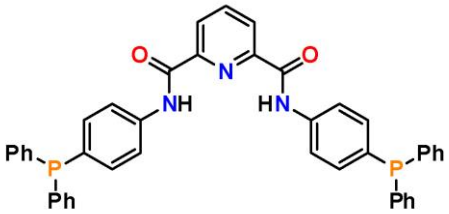

L2

N^2,N^6-Bis(3-(diphenylphosphino)phenyl)pyridine-2,6-dicarboxamide (L1)

3-diphenylphosphinoaniline (1.659 g, 5.983 mmol) and 2,6-pyridinedicarboxylic acid (0.50 g, 2.991 mmol) were dissolved in 5 mL of pyridine and stirred over an oil bath maintained at 100 ˚C for 15 min. To the reaction mixture, triphenylphosphite (1.949 g, 6.282 mmol) was added drop-wise and the reaction mixture was stirred for 6 h at 80 ˚C. After cooling the reaction mixture to room temperature solvent was removed under reduced pressure to afford an oily product. This product was washed thrice with cold water and triturated with cold acetonitrile that resulted in a white solid. This product was further washed with cold acetonitrile, filtered and dried under vacuum. Yield: 1.80 g (88 %). $C_{43}H_{33}N_3O_2P_2$ (685.69): Calcd. C 75.32; H 4.85; N 4.13, Found: C 75.10; H 4.82; N 4.11. FTIR spectrum (Zn-Se ATR): 3284 (ν_{NH}), 3101, 3066, 3047, 2917, 2848 (ν_{CH}), 1681 ($\nu_{C=O\ asym.}$), 1594 ($\nu_{C=O\ sym.}$), 1665, 1581, 1548, 1529 ($\nu_{C=C}$), 745 ($\nu_{CH\ bending}$) cm^{-1}. ^1H NMR spectrum (400 MHz, DMSO-D6) δ 10.98 (s, 2H, -NH), 8.32 – 8.28 (m, 2H, H^2), 8.23 (t, *J* = 6.9 Hz, 1H, H^1), 7.87 –7.92 (m, 4H, H^3 and H^6), 7.47 (t, *J* = 7.8 Hz, 2H, H^4), 7.32 – 7.42 (m, 12H, H^8 and H^9), 7.22 – 7.32 (dd, *J* = 8.9, 5.3 Hz, 8H, H^7), 6.97 (t, *J* = 7.2 Hz, 2H, H^5) ppm. ^{13}C NMR spectrum (100 MHz, DMSO-D6) δ 162.29 (C4), 149.18 (C3), 140.49 (C1), 139.0 (C5), 138.05 (C9), 137.93 (C11), 137.01 (C7), 136.90 (C14), 133.99 (C8), 133.79 (C10), 129.62 (C2), 129.40 (C12), 129.34 (C16), 126.17 (C13), 125.98 (C15), 122.12 (C6) ppm. ^{31}P NMR spectrum (162 MHz, DMSO-D6) δ – 4.61 ppm.

N^2,N^6-Bis(4-(diphenylphosphino)phenyl)pyridine-2,6-dicarboxamide (L2)

A similar procedure as outlined for L1 was followed with following reagents: 4-diphenylphosphinoaniline (1.659 g, 5.983 mmol), 2,6-pyridinedicarboxylic acid (0.50 g, 2.991 mmol), triphenylphosphite (1.949 g, 6.282 mmol). Yield: 1.82 g (89 %). $C_{43}H_{33}N_3O_2P_2$ (685.69): Calcd. C 75.32, H 4.85, N 4.13, Found: C 75.28; H 4.65; N 4.40. FTIR spectrum (Zn-Se ATR): 3294 (ν_{NH}), 3102, 3063, 3046, 3029, 3003 (ν_{CH}), 1683 ($\nu_{C=O\ asym.}$), 1592 ($\nu_{C=O\ sym.}$), 1664, 1578, 1531, 1512 ($\nu_{C=C}$), 745 ($\nu_{CH\ bending}$) cm^{-1}. ^1H NMR spectrum (400 MHz, DMSO-D6) δ 11.07 (s, 2H, NH), 8.36 (d, *J* = 7.4 Hz, 2H, H^2), 8.31 – 8.24 (t, 1H, H^1), 7.92 (d, *J* = 8.1 Hz, 4H, H^3), 7.37 (d, *J* = 3.9 Hz, 12H, $H^{6,7}$), 7.32 – 7.26 (m, 4H, H^4), 7.25 – 7.18 (m, 8H, H^5) ppm. ^{13}C NMR spectrum (50 MHz, DMSO) δ = 161.75 (C4), 148.64 (C3), 138.85 (C1), 136.82 (C5), 133.31 (C7), 132.93 (C9), 131.58 (C8), 128.91 (C10), 128.83 (C11), 128.69 (C12), 125.46 (C2), 121.07 (C6). ^{31}P NMR spectrum (162 MHz, DMSO-D6) δ – 7.34 ppm.

3. Synthesis of Palladium Macrocycles

Synthesis of Pd-macrocycle 1. Ligand L1 (0.080 g, 0.116 mmol) and [$Pd(MeCN)_2Cl_2$] (0.03 g, 0.116 mmol) were dissolved in 15 mL of CH_2Cl_2 and stirred for 2 h at room temperature. The solvent was evaporated under reduced pressure and the crude orange product was isolated after washing with cold diethyl ether. Crystallization was achieved by layering the CH_2Cl_2 solution of compound with CH_3CN. This afforded a highly crystalline product within 2–3 days that was filtered, washed with diethyl ether, and dried under vacuum. Yield: 0.098g (97 %). $C_{44}H_{34.5}Cl_2N_{3.5}O_2P_2Pd$ (883.540 including 0.5 CH_3CN): Calcd. C 59.81, H 3.94, N 5.55, Found: C 59.99; H 3.58; N 5.50. FTIR spectrum (Zn-Se ATR): 3367 (ν_{NH}), 3054, 2973, 2926, 2866 (ν_{CH}), 1696 ($\nu_{C=O\ asym.}$), 1593, 1541 ($\nu_{C=C}$), 744 ($\nu_{CH\ bending}$) cm^{-1}. UV/Vis spectrum (EtOH): λ_{max} (ε, 20 $\mu M^{-1}cm^{-1}$) = 285 (0.473), 340 (0.359). ^1H NMR spectrum (400 MHz, $CDCl_3$) δ 10.53 (s, 2H, NH), 8.78 (t, *J* = 7.2 Hz, 2H, H^6), 8.65 (d, *J* = 8.0 Hz, 2H, H^3), 8.46 (d, *J* = 8.0 Hz, 2H, H^2), 8.22 (t, *J* = 7.7 Hz, 1H, H^1), 7.57 (dd, *J* = 12.2, 5.7 Hz, 8H, H^7), 7.48 – 7.33 (m, 14H, $H^{4,8,9}$), 7.10 – 7.00 (m, 2H, H^5) ppm. ^{13}C NMR spectrum (100 MHz, $CDCl_3$) δ 160.18 (C4), 147.87 (C3), 140.78 (C1), 134.65 (C5), 134.42 (C6), 134.36 (C9), 134.30 (C11), 130.11 (C8), 129.89 (C10), 128.18 (C7), 128.13 (C13), 128.08 (C14), 125.0 (C2), 120.88 (C6) ppm. ^{31}P NMR spectrum (162 MHz, $CDCl_3$) δ 25.87 ppm.

Synthesis of Pd-macrocycle 2. A similar procedure as outlined for **1** was adopted with the following reagents: L2 (0.080 g, 0.116 mmol), $[Pd(MeCN)_2Cl_2]$ (0.03 g, 0.116 mmol). Single crystal suitable for diffraction studies were grown by the vapour diffusion of diethyl ether to a mixture of DMF – MeOH (4:1) solution. Yield: 0.100 g (99 %). $C_{93}H_{84}Cl_4N_8O_7P_4Pd_2$ (1904.22 including 2DMF + 1MeOH): Calcd. C 58.66, H 4.45, N 5.88, Found: C 58.18; H 4.43; N 5.59. FTIR spectrum (Zn-Se ATR): 3294 (ν_{NH}), 3054, 2922, 2858 (ν_{CH}), 1681 ($\nu_{C=O\ asym.}$), 1668, 1594, 1580, 1514 ($\nu_{C=C}$), 745 ($\nu_{CH\ bending}$) cm^{-1}. UV/Vis (EtOH): λ_{max} (ε, $M^{-1}cm^{-1}$) = 285 (0.795). ^1H NMR spectrum (400 MHz, DMSO-D6) δ 11.10 (s, 2H, NH), 8.27 (d, J = 18.2 Hz, 5H, $H^{1,3,4}$), 7.92 (d, J = 6.0 Hz, 2H, H^2), 7.58 (dd, J = 42.1, 35.9 Hz, 25H, $H^{7,5,6}$) ppm. ^{13}C NMR spectrum (100 MHz, DMSO-D6) δ 162.40 (C4), 148.99 (C3), 140.61 (C1), 138.27 (C5), 135.14 (C7), 135.03 (C9), 132.00 (C10), 129.39 (C8), 128.95 (C12), 128.84 (C11), 126.09 (C2), 124.12 (C6). ^{31}P NMR spectrum (162 MHz, DMSO-D6) δ 32.66 ppm.

4. Physical Measurements

Elemental analysis data were obtained by Elementar Analysen Systeme GmbH Vario EL-III instrument. The ^1H, ^{13}C and ^{31}P NMR spectra recorded with a JEOL 400 MHz instrument. The FTIR spectra (Zn–Se ATR) were recorded with a Perkin-Elmer Spectrum-Two spectrometer. The absorption spectra were recorded with a Perkin-Elmer Lambda 25 spectrophotometer. Fluorescence studies were performed with a Cary Eclipse Fluorescence Spectrophotometer. ESI-MS mass spectra were measured either with Agilent mass spectrometer or using an AB SCIEX 5800 MALDI TOF/TOF^{TM} system with LC-MALDI. Florescence lifetime measurements were performed with Fluoro Time 300 (Pico Quant, Berlin, Germany). All absorption and fluorescence spectral studies were performed with a 1.0 cm pathlength cuvette at room temperature.

5. Determination of Constants

Stern-Volmer Constant (K_{SV}) and Detection Limit. Fluorescence titrations were further evaluated using the Stern–Volmer equation [equation (1)].[3]

$$I_0/I = 1 + K_{SV}[PA] \qquad (1)$$

where I_0 is the emission intensity of Pd-macrocycles **1** and **2** at 432 nm and 428 nm, respectively in the absence of PA (picric acid), I is the emission intensity in the presence of PA and K_{SV} is the Stern–Volmer constant.

The detection limit was calculated using equation (2),

Detection limit: $3\sigma/k$ (2)

where σ is the standard deviation of ten blank replicate measurements and k is the slope of a plot of fluorescence intensity of **1** and **2** at 432 nm and 428 nm, respectively versus picric acid concentration.[4]

Binding Stoichiometry and the Binding Constant (K_b). The binding stoichiometry of picric acid with Pd-macrocycles **1** and **2** was determined by the Job's plot.[5] The binding constant (K_b) for the binding of Pd-macrocycle **1** and **2** with picric acid were determined by the Benesi-Hildebrand equation. The binding constant K_b was calculated graphically by plotting $1/(I\text{-}I_0)$ against 1/[PA].[5]

$$1/(I\text{-}I_0) = 1/\{K_b(I_0 - I_{min})[PA]\} + 1/(I_0 - I_{min}) \quad (3)$$

Where I is the fluorescence intensity of **1** and **2** in presence of PA, I_0 is the intensity of **1** and **2** in absence of PA and I_{min} is the minimum fluorescence intensity in presence of PA. The plot $1/(I\text{-}I_0)$ vs. 1/[PA] were linearly fitted and the K_b value was obtained from the slope and intercept of the line.

6. Crystallography

The X-ray diffraction intensity data were collected at 298 K with an Oxford XCalibur Sapphire3 CCD diffractometer equipped with graphite monochromatic Mo-$K\alpha$ radiation (λ = 0.71073 Å).[6] Data reduction was performed with CrysalisPro program (Oxford Diffraction ver. 171.34.40).[6] Multi-scan absorption correction was applied to all complexes. The structures were solved by direct methods using SIR-92[7] and refined by full-matrix least-squares refinement techniques on F^2 using SHELXL-2016/4.[8] The non-hydrogen atoms were anisotropically refined whereas the hydrogen atoms were placed at calculated positions and included in the last cycles of the refinement. All calculations were carried out with the WinGX crystallographic package.[9] In case of macrocycle **2**, the oxygen atom of methanol molecule (O5) was disordered and thus O5 atom was refined isotropically. In addition, no hydrogen atom was assigned to O5 atom due to the presence of disorder. The crystallographic data collection and structure solution parameters are presented in Table S4. CCDC-1582152 and 1582153 contain the supplementary crystallographic data for this paper. This data can be obtained free of charge from The Cambridge Crystallographic Data Center via www.ccdc.cam.uk/data_request/cif.

7. Fabrication of Filter Paper Test Strips

Strips of Whatman filter paper were dipped in an ethanol solution of fluorescent Pd-macrocycle **2** and were air-dried.[10] Test strips were then dipped directly for a few seconds into an aqueous solution of picric acid of different concentrations. Such paper strips were then investigated under visible and ultraviolet light.

8. Abbreviations Used for Various Substrates

Benzoic acid (BA), nitroethane (NE), nitrobenzene (NB), 1,3-dinitrobenzene (1,3-DNB), 1,4-dinitrobenzene (1,4-DNB), 1,3,5-trinitroperhydro-1,3,5-triazinane (RDX), 4-nitrotoluene (4-NT), 2,4-dinitrotoluene (2,4-DNT), 2,4,6-trinitrotoluene (TNT), 2-nitroaniline (2-NA), 3-nitroaniline (3-NA), 4-nitroaniline (4-NA), 2-nitrophenol (2-NP), 3-nitrophenol (3-NP), 4-nitrophenol (4-NP), 2,4-dinitrophenol (2,4-DNP), picric acid (PA).

9. References

1. Dwyer, A. N.; Grossel, M. C.; Horton, P. N. Binding of Co^{3+} and within a Pyridine-cored Molecular Cleft. *Supramol. Chem.* **2004**, *16*, 405-410.
2. Ganguly, A.; Paul, B. K.; Ghosh, S.; Kar, S.; Guchhait, N. Selective fluorescence sensing of Cu(II) and Zn(II) using a new Schiff base-derived model compound: naked eye detection and spectral deciphering of the mechanism of sensory action. *Analyst* **2013**, *138*, 6532-6541.
3. Liang, C.; Bu, W.; Li, C.; Men, G.; Deng, M.; Jiangyao, Y.; Sun, H.; Jiang, S. A highly selective fluorescent sensor for Al^{3+} and the use of the resulting complex as a secondary sensor for PPi in aqueous media: its applicability in live cell imaging. *Dalton Trans.* **2015**, *44*, 11352-11359.
4. Senthilvelan, A.; Ho, I.; Chang, K.; Lee, G.; Liu, Y.; Chung, W. Cooperative Recognition of a Copper Cation and Anion by a Calix[4]arene Substituted at the Lower Rim by a β-Amino-α,β-Unsaturated Ketone. *Chem. Eur. J.* **2009**, *15*, 6152-6160.
5. Benesi, H. A.; Hildebrand, J. H. A Spectrophotometric Investigation of the Interaction of Iodine with Aromatic Hydrocarbons. *J. Am. Chem. Soc.* **1949**, *71*, 2703-2707.
6. CrysAlisPro, v. 1.171.33.49b, Oxford Diffraction Ltd., **2009**.
7. Altomare, A.; Cascarano, G.; Giacovazzo, C.; Guagliardi, A. Completion and refinement of crystal structures with SIR92. *J. Appl. Crystallogr.* **1994**, *27*, 343-350.

8. Sheldrick, G. M. A short history of SHELX. *Acta Crystallogr. Sect. A: Found. Crystallogr.* **2008**, *64*, 112-122.
9. Farrugia, L. J. WinGX, v2014.1, An Integrated System of Windows Programs for the Solution, Refinement and Analysis of Single- Crystal X-ray Diffraction Data, Department of Chemistry, University of Glasgow, **2014**.
10. Bansal, D.; Gupta, R. Chemosensors Containing Appended Benzothiazole group(s): Selective Binding of Cu^{2+} and Zn^{2+} Ions by Two Related Receptors. *Dalton Trans.* **2016**, *45*, 502 – 507.

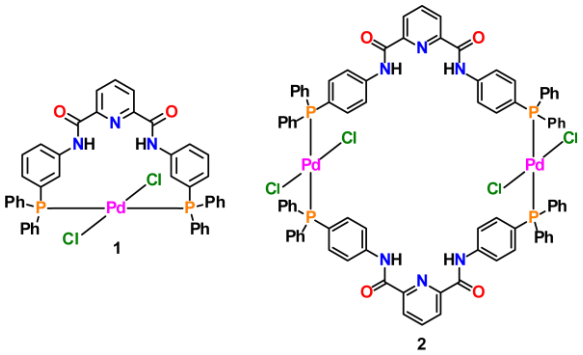

Scheme S1. Palladium macrocycles **1** and **2** used and discussed in this work.

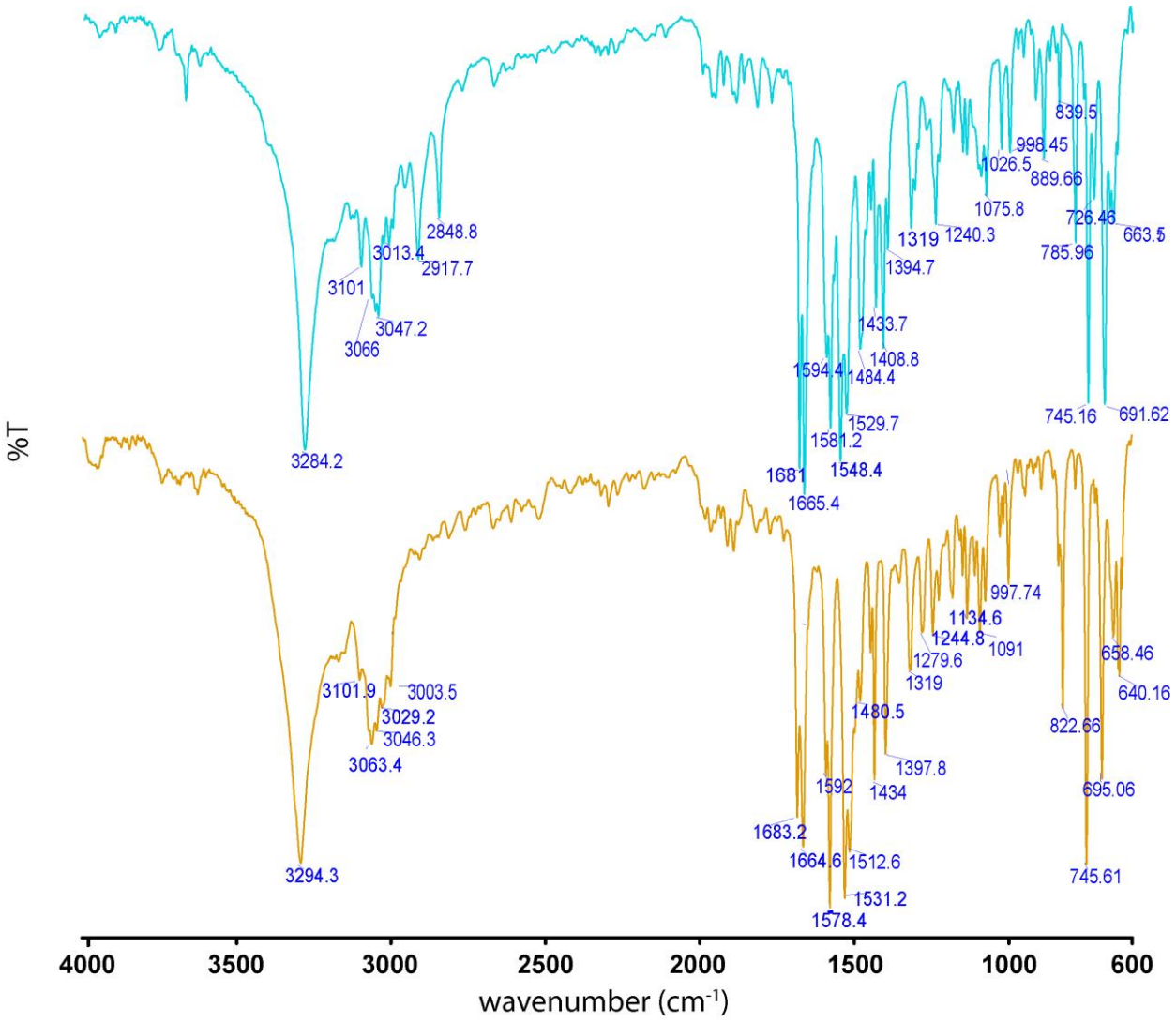

Figure S1. FTIR spectra of ligands L1 (cyan trace) and L2 (orange trace).

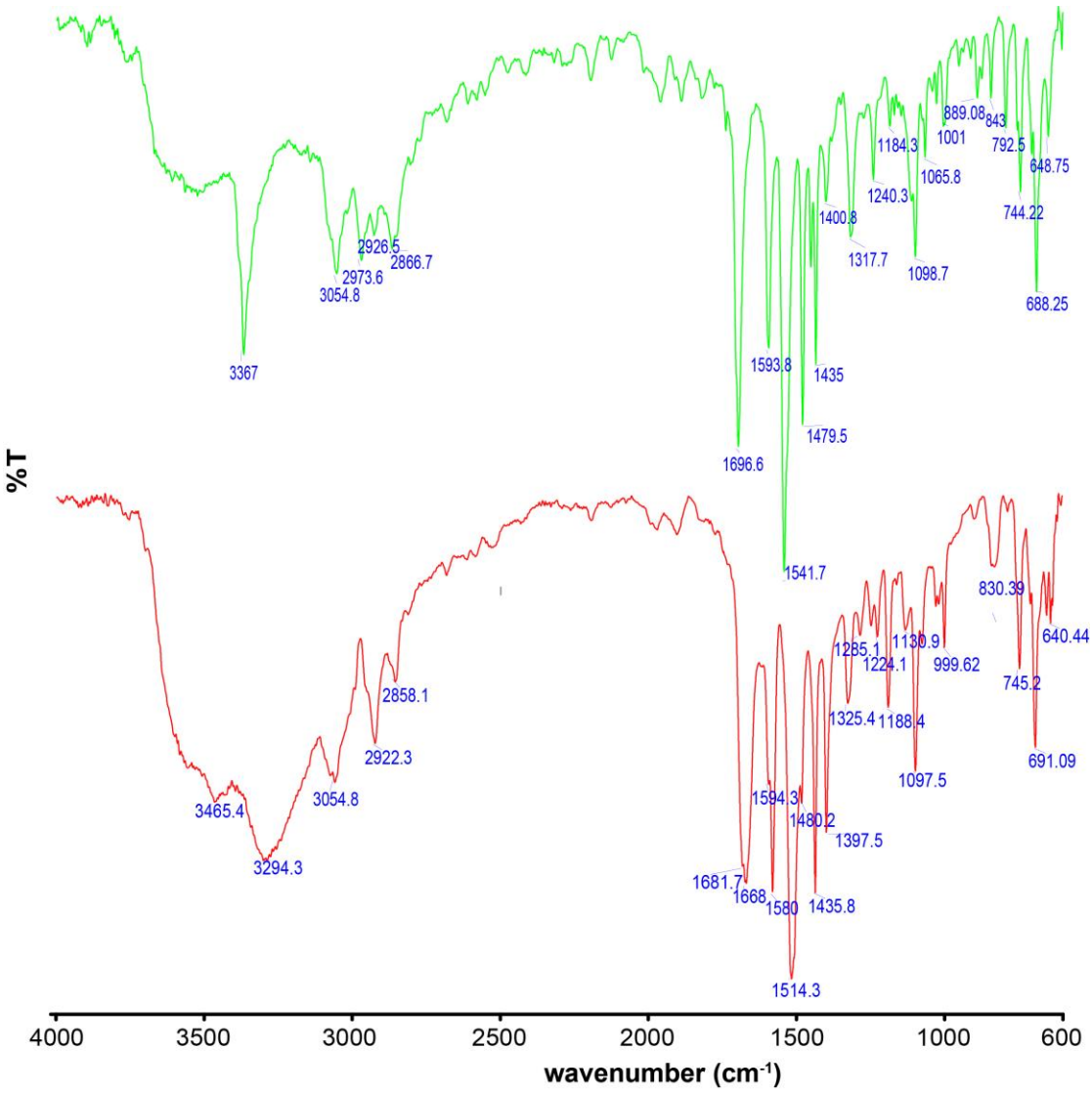

Figure S2. FTIR spectra of Pd-macrocycles **1** (green trace) and **2** (red trace).

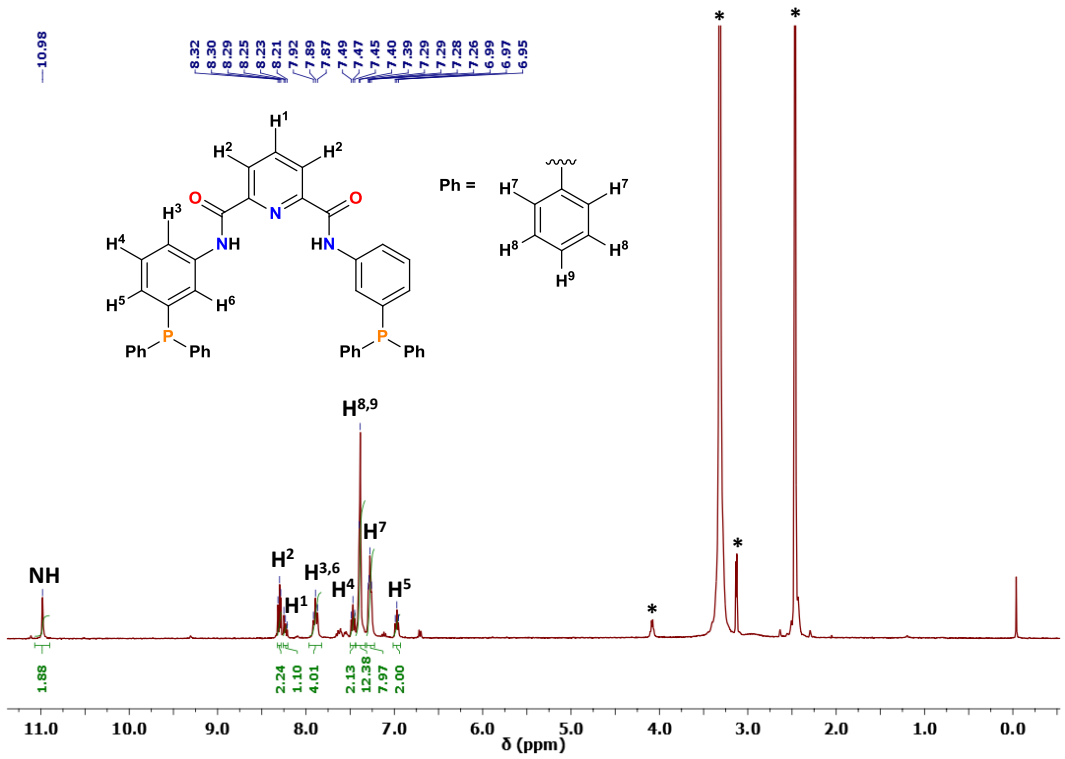

Figure S3. ^{1}H NMR spectrum of L1 recorded in DMSO-D_6. Asterisk represents the residual solvent and adventitious water.

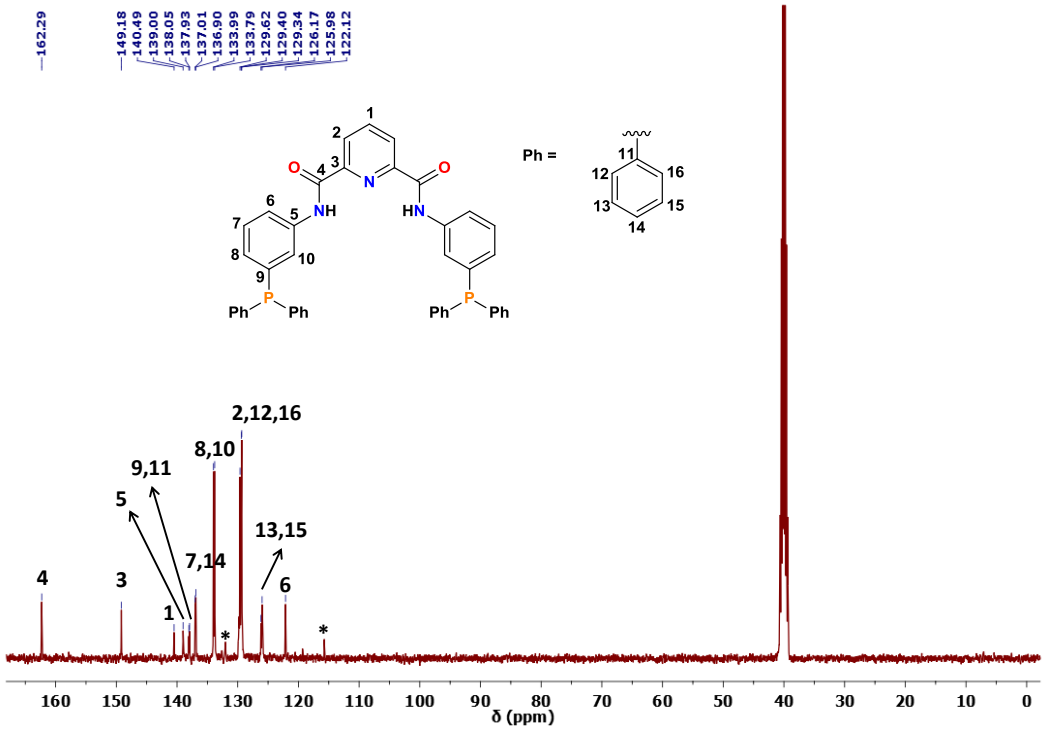

Figure S4. ^{13}C NMR spectrum of L1 recorded in DMSO-D_6. Asterisk represents the residual solvent and some unknown impurities.

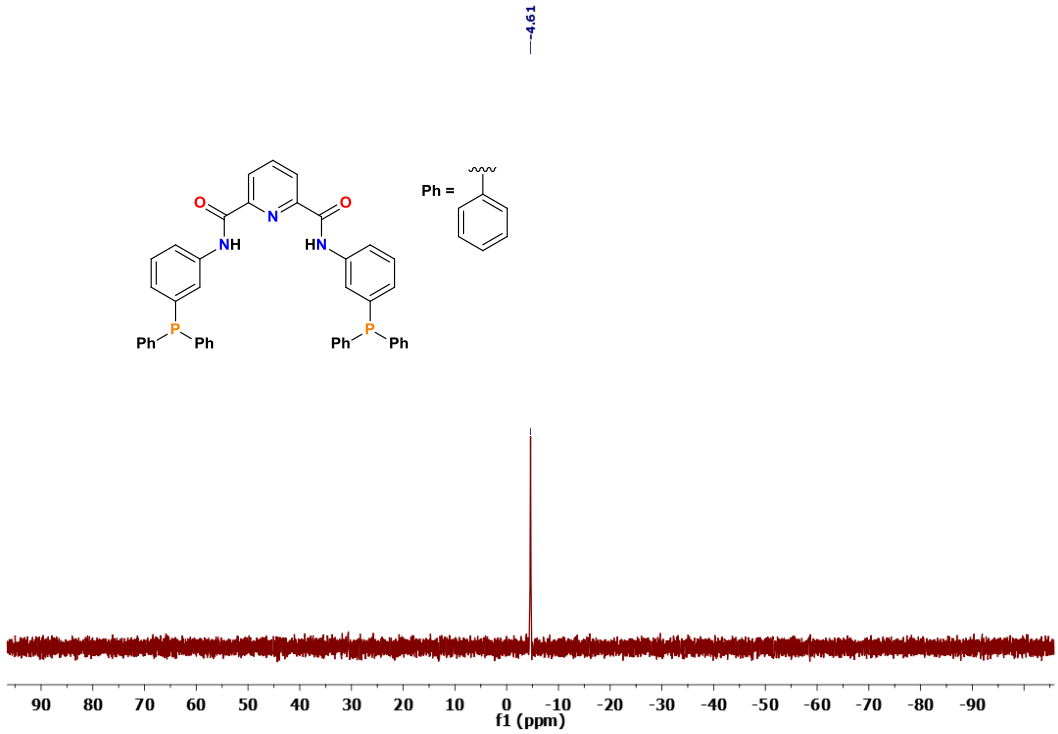

Figure S5. ^{31}P NMR spectrum of L1 recorded in DMSO-D_6.

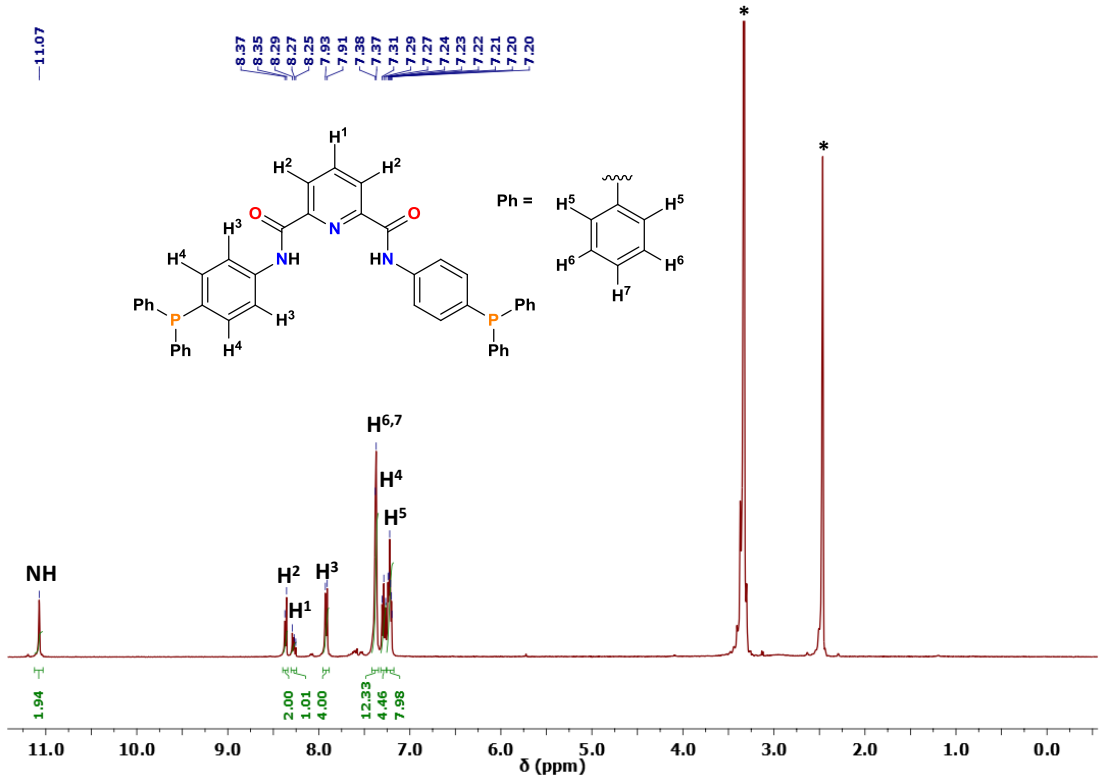

Figure S6. ^{1}H NMR spectrum of L2 recorded in DMSO-D_6. Asterisk represents the residual solvent and adventitious water.

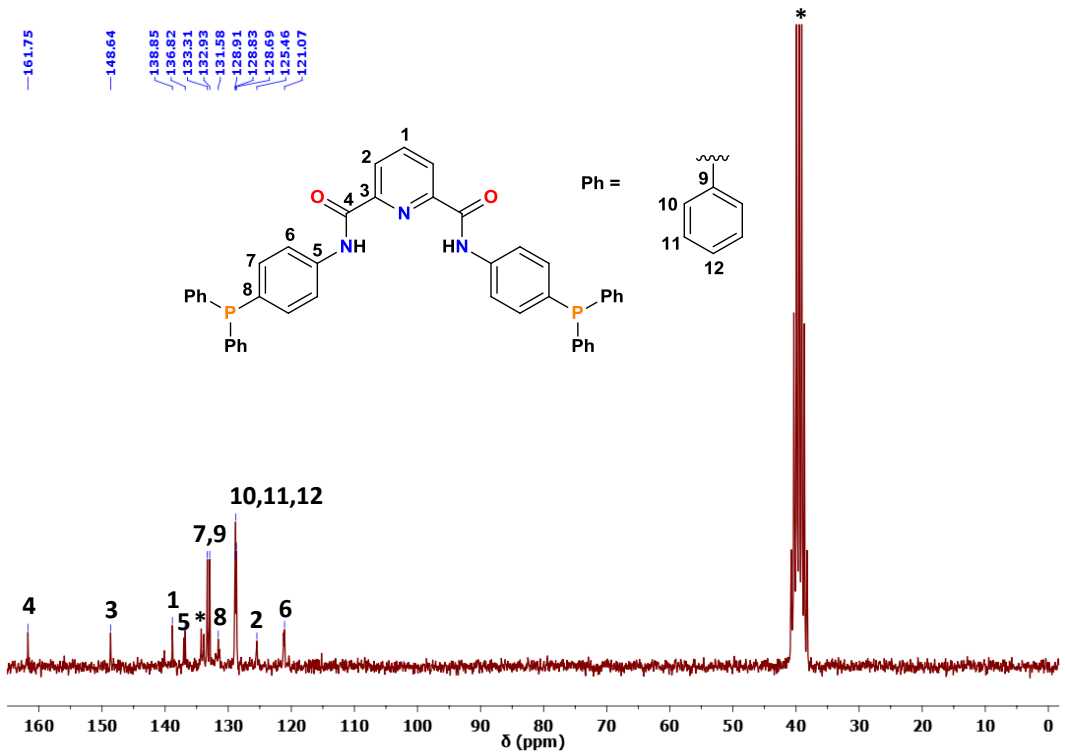

Figure S7. ^{13}C NMR spectrum of L2 recorded in DMSO-D_6. Asterisk denotes the residual solvent and pyridine.

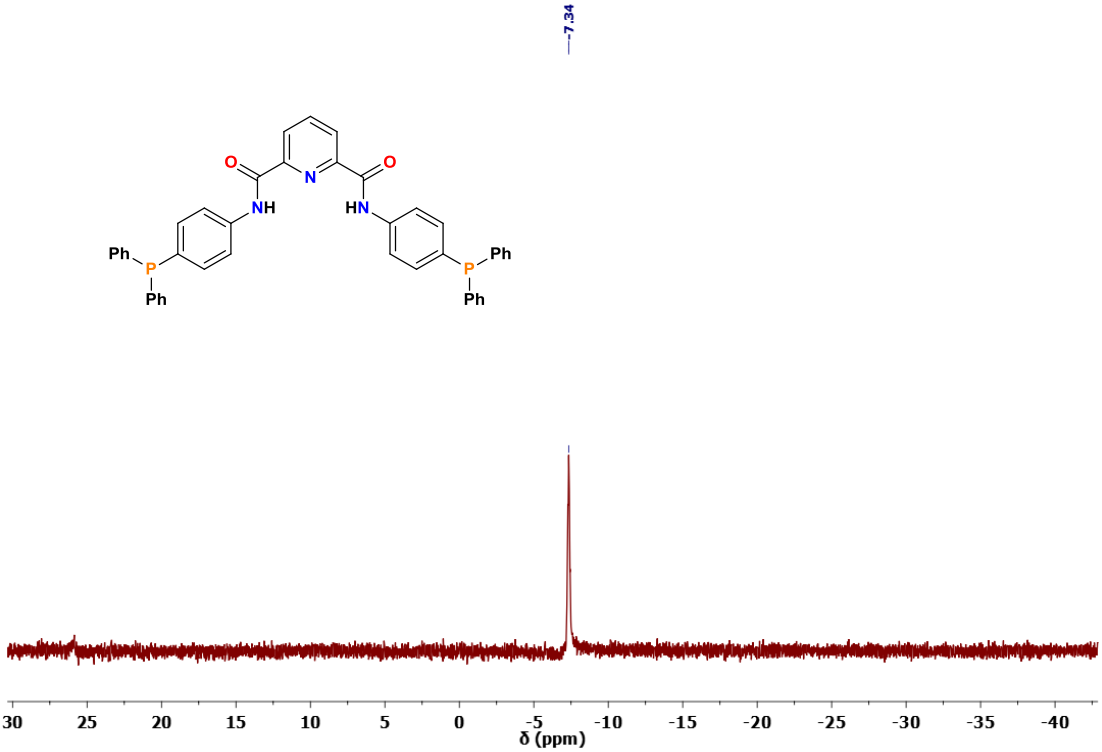

Figure S8. ^{31}P NMR spectrum of L2 recorded in DMSO-D_6.

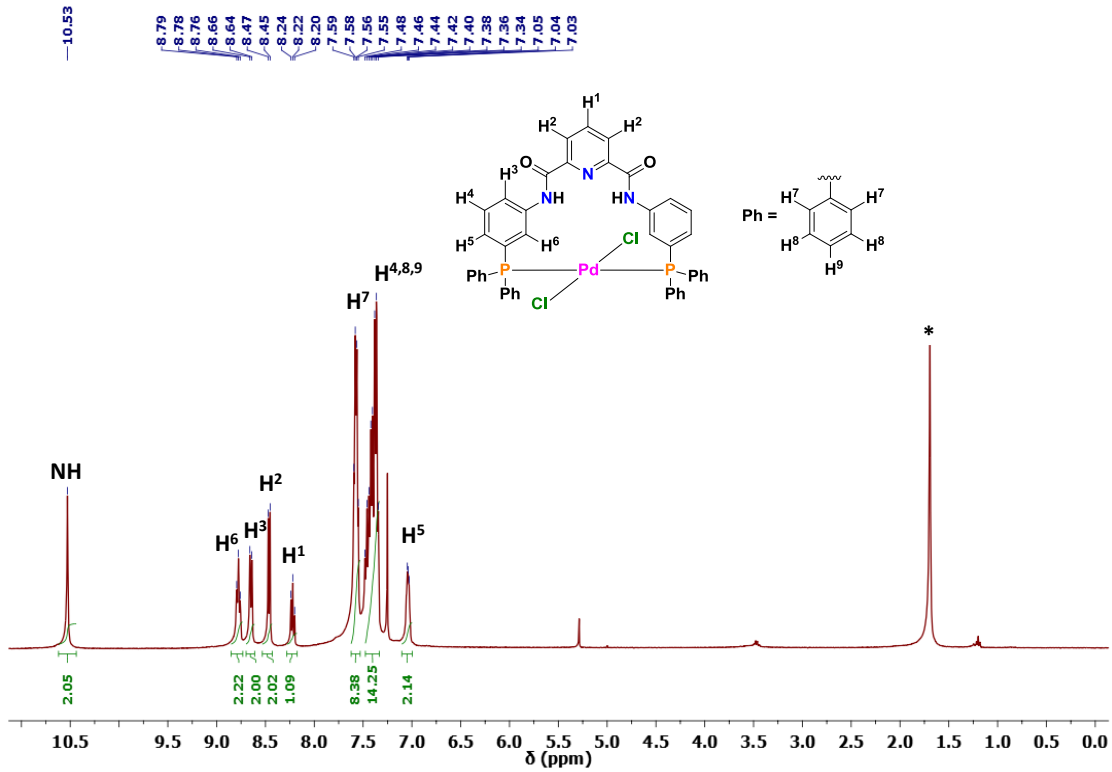

Figure S9. ^{1}H NMR spectrum of Pd-macrocycle **1** recorded in $CDCl_3$. Asterisk represents the adventitious water in the NMR solvent.

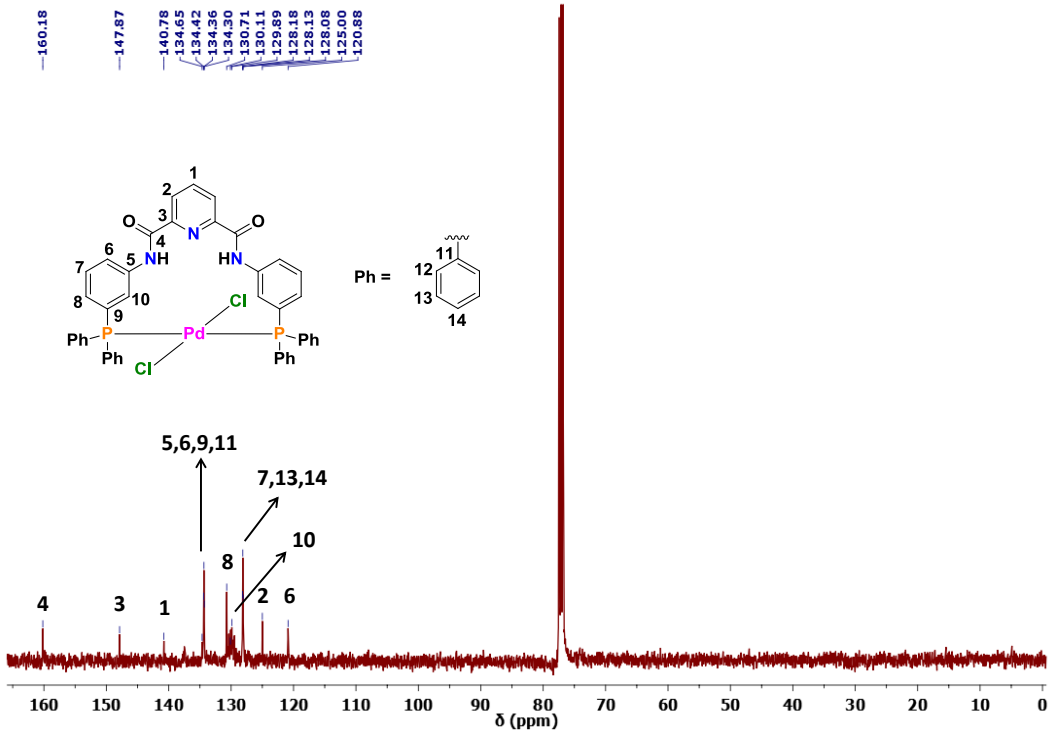

Figure S10. ^{13}C NMR spectrum of Pd-macrocycle **1** recorded in $CDCl_3$.

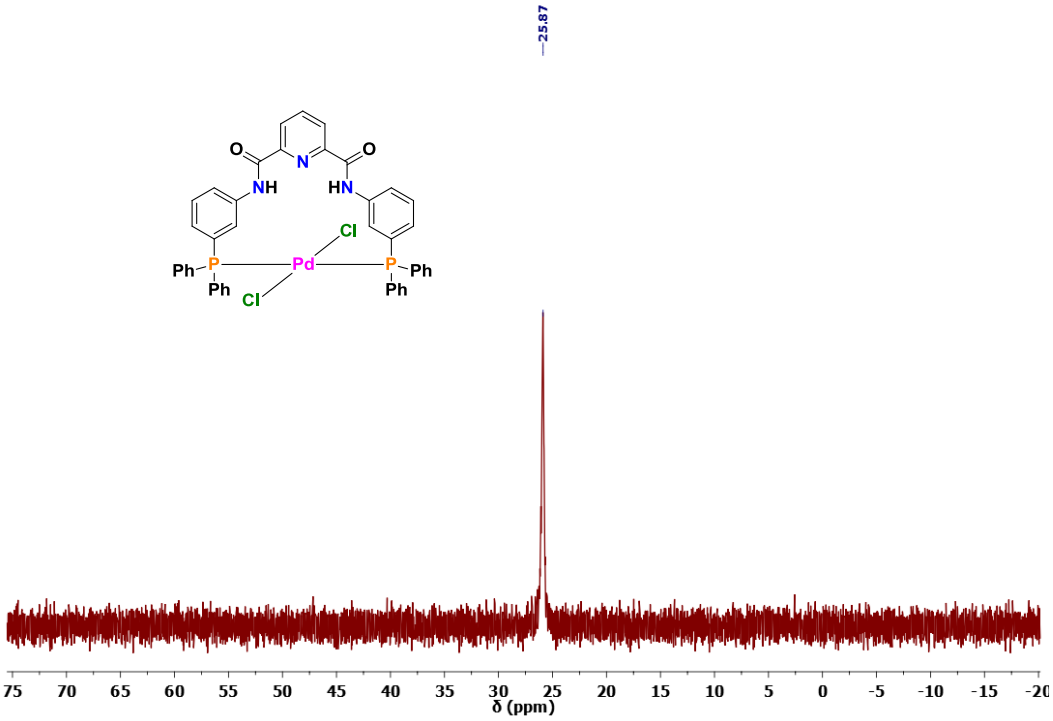

Figure S11. ^{31}P NMR spectrum of Pd-macrocycle **1** recorded in $CDCl_3$.

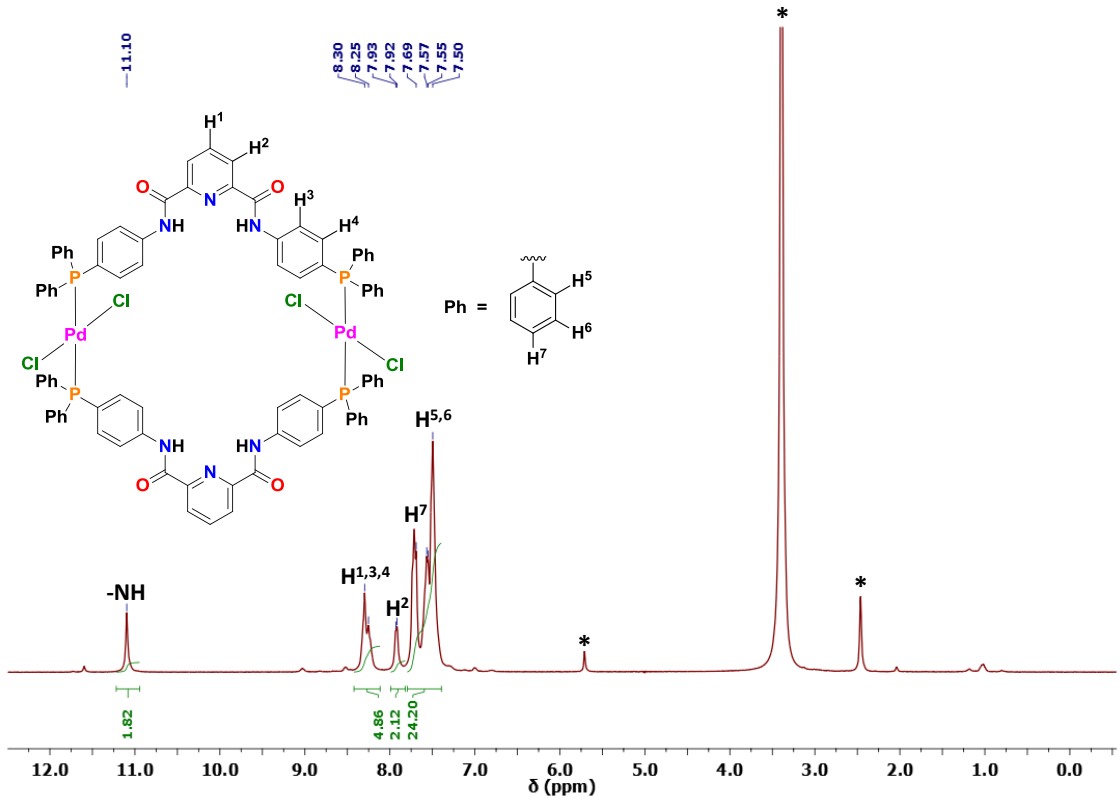

Figure S12. ^{1}H NMR spectrum of Pd-macrocycle **2** recorded in DMSO-D_6. Asterisk represents the residual solvent and CH_2Cl_2.

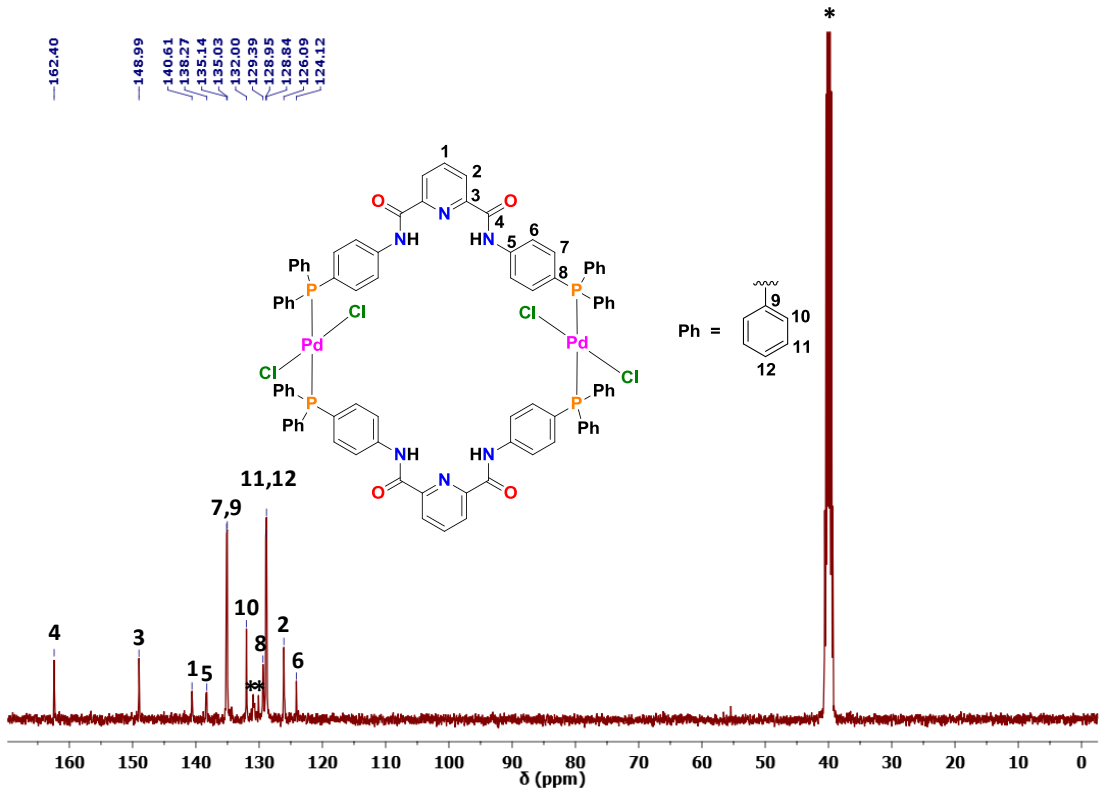

Figure S13. ^{13}C NMR spectrum of Pd-macrocycle **2** recorded in DMSO-D_6. Asterisk represents the residual solvent and some unknown impurities.

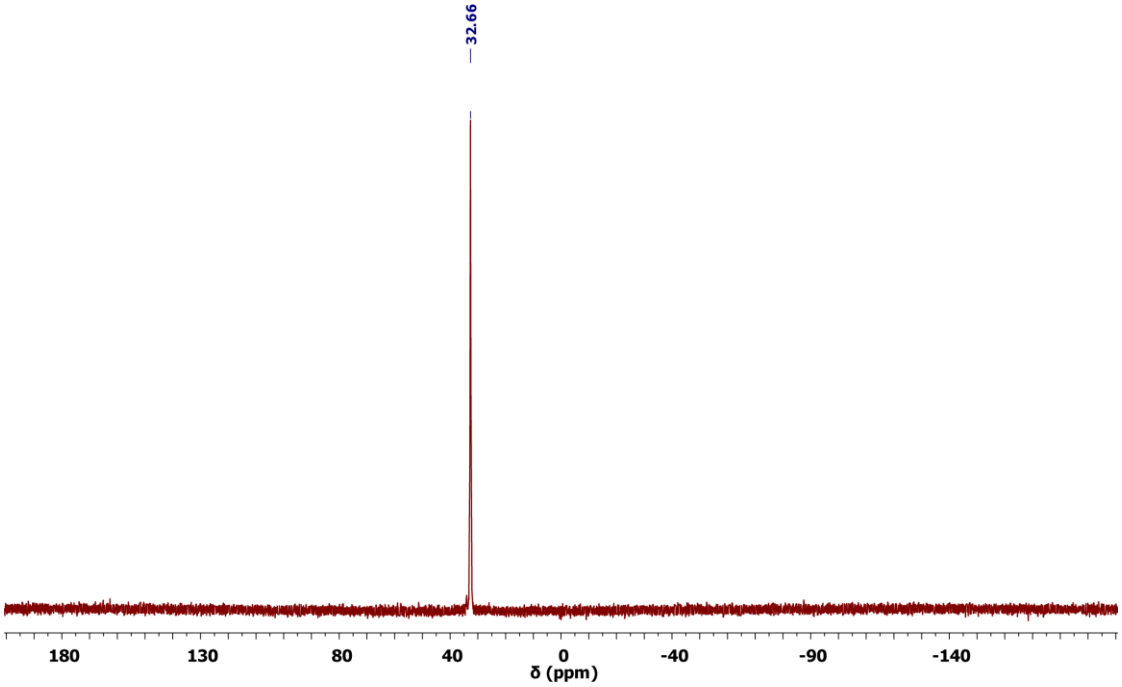

Figure S14. ^{31}P NMR spectrum of Pd-macrocycle **2** recorded in DMSO-D_6.

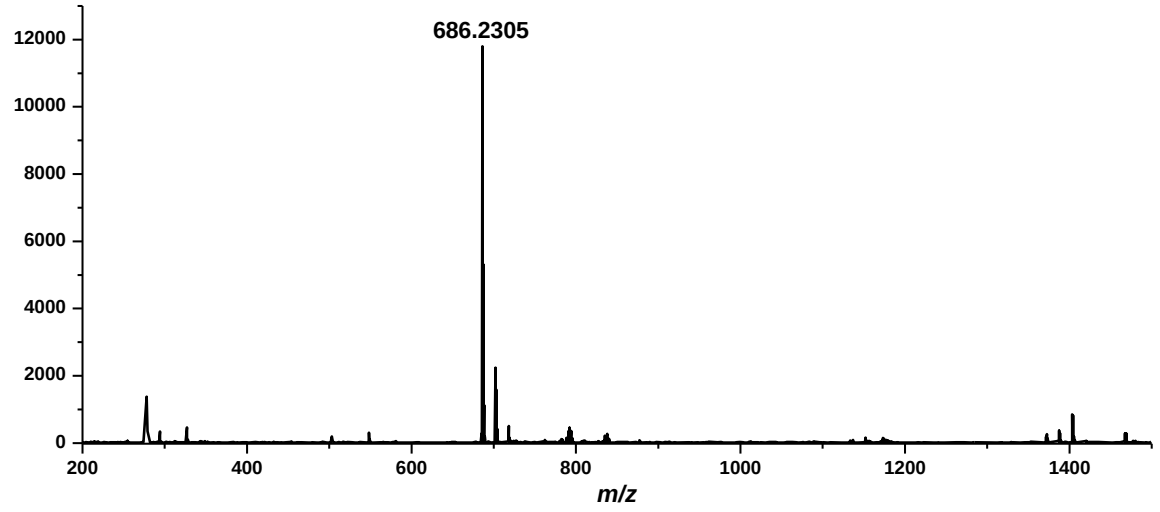

Figure S15. ESI^+-MS spectrum of ligand L1 recorded in $CHCl_3$.

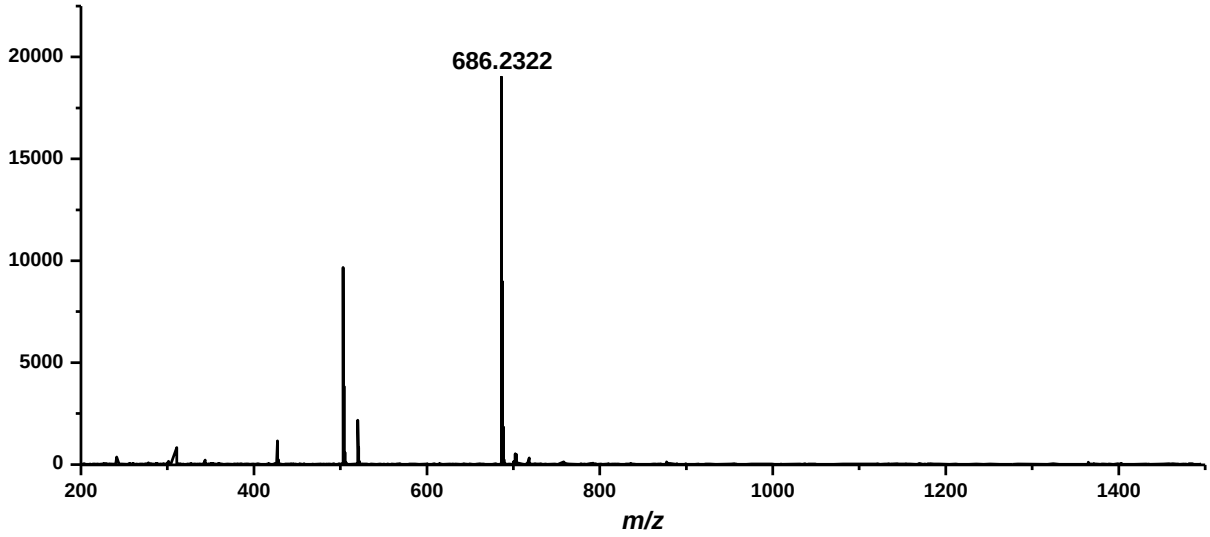

Figure S16. ESI^+-MS spectrum of ligand L2 recorded in $CHCl_3$.

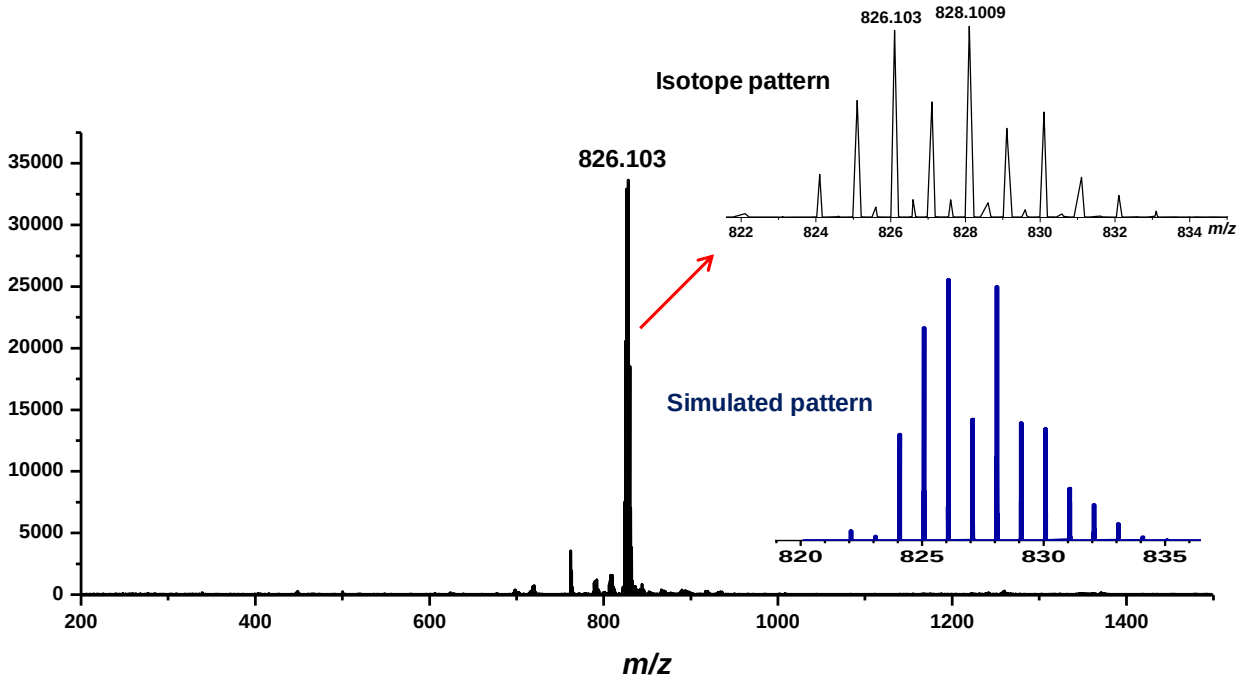

Figure S17. ESI^+-MS spectrum of Pd-macrocycle **1** (recorded in $CHCl_3$) with its experimental isotope pattern and the simulated pattern calculated using ChemCalc.

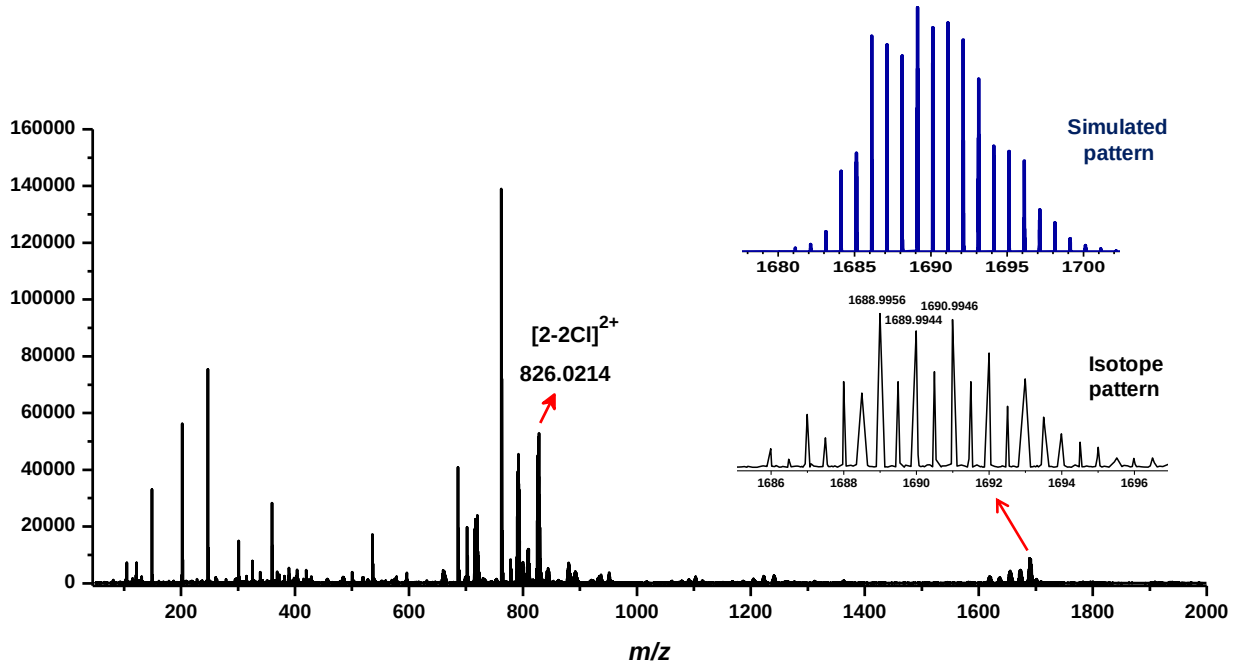

Figure S18. ESI^+-MS spectrum of Pd-macrocycle **2** (recorded in $CHCl_3$) with its experimental isotope pattern and the simulated pattern calculated using ChemCalc.

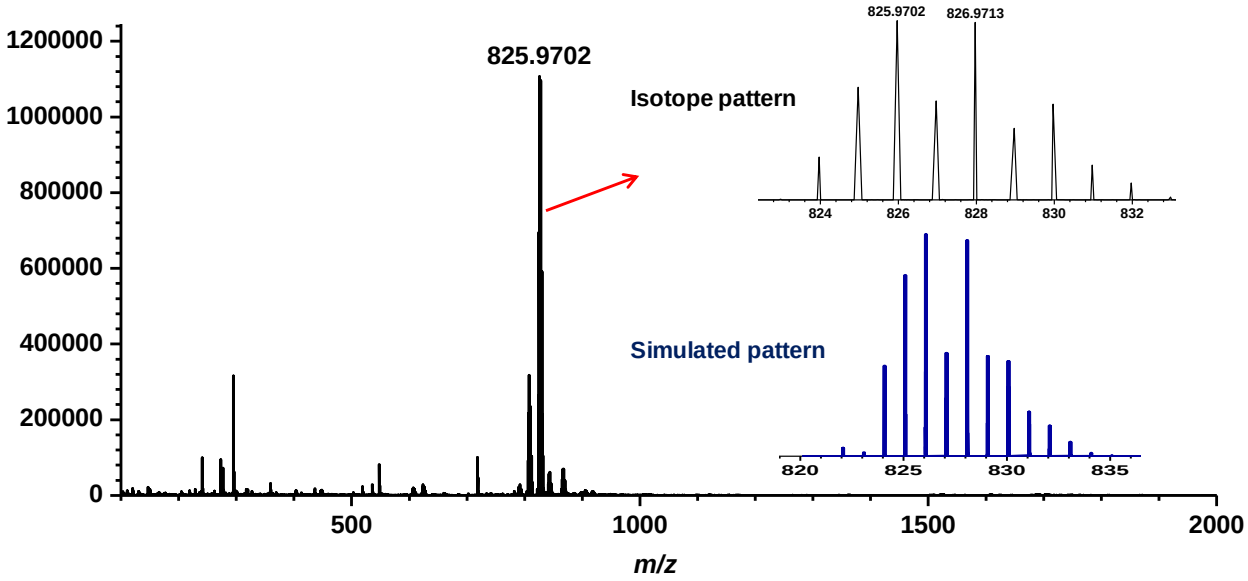

Figure S19. ESI$^+$-MS spectrum of Pd-macrocycle **1** (recorded in EtOH) with its experimental isotope pattern and the simulated pattern calculated using ChemCalc.

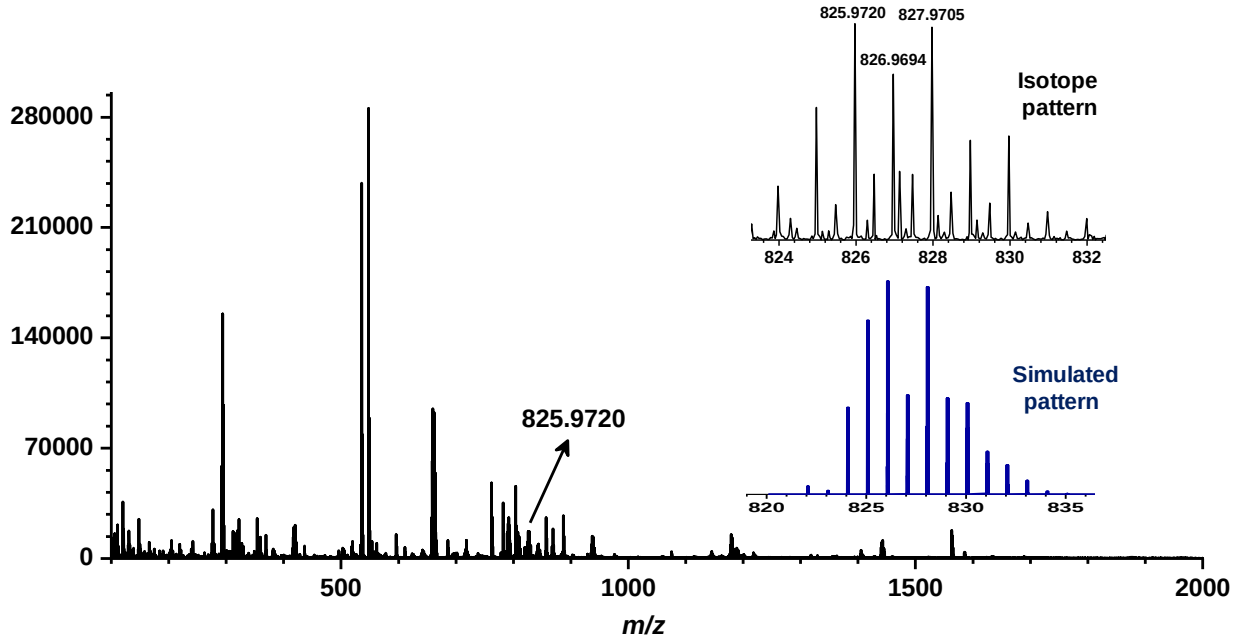

Figure S20. ESI$^+$-MS spectrum of Pd-macrocycle **2** (recorded in EtOH) with its experimental isotope pattern and the simulated pattern calculated using ChemCalc.

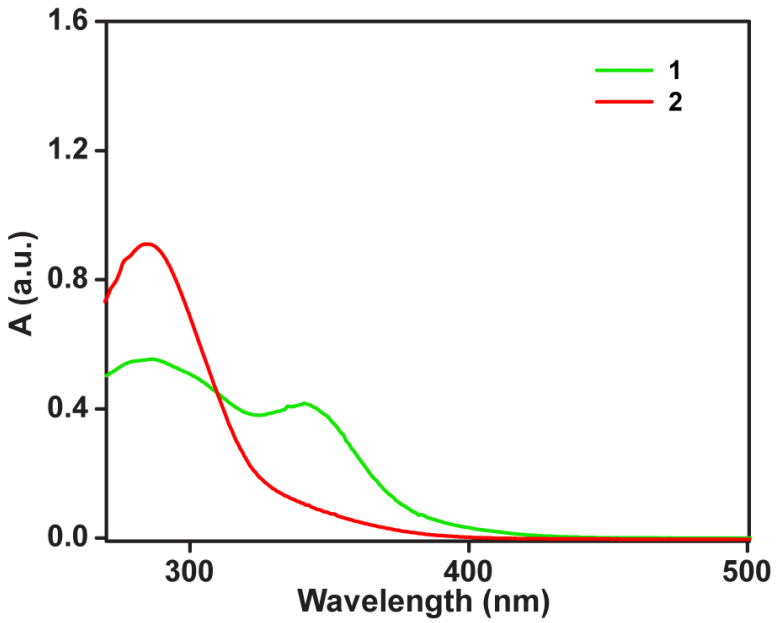

Figure S21. Absorption spectra of Pd-macrocycles **1** and **2** recorded in EtOH.

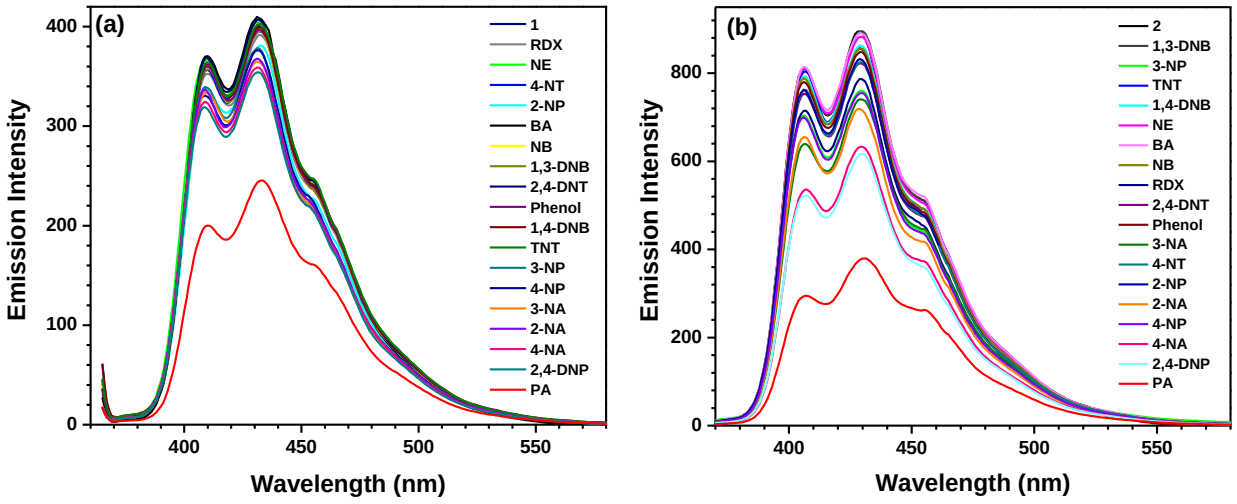

Figure S22. Emission spectra of (a) Pd-macrocycles **1** and (b) **2** (1 μM) after addition of different nitro-aromatic compounds (0-20 μM) in EtOH.

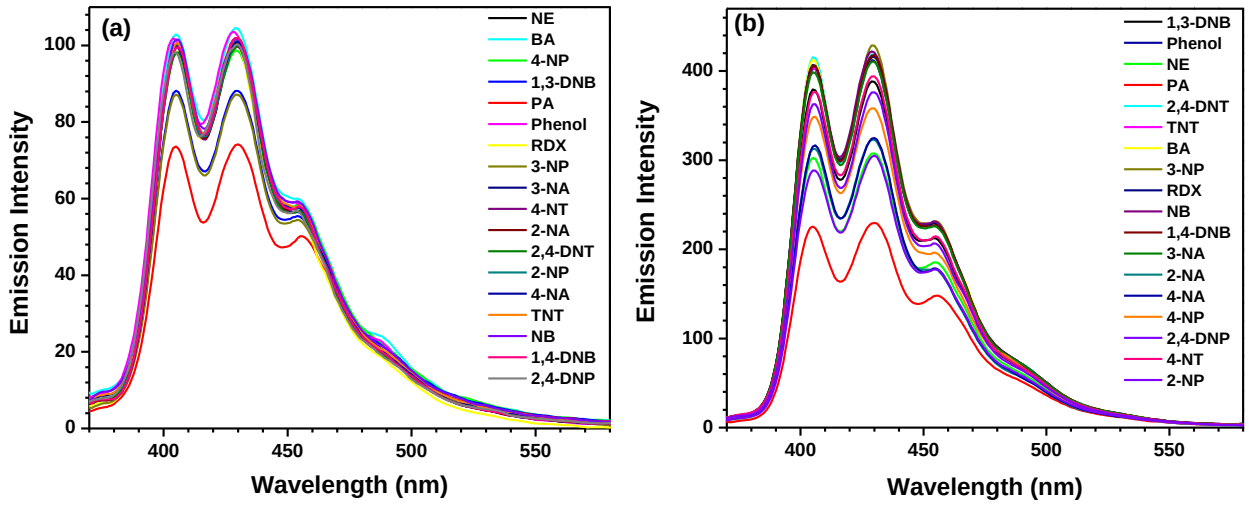

Figure S23. Change in emission of Pd-macrocycles (a) **1** and (b) **2** (1μM) in presence of NACs (20 μM) (λ_{ex} = 350 nm) in THF.

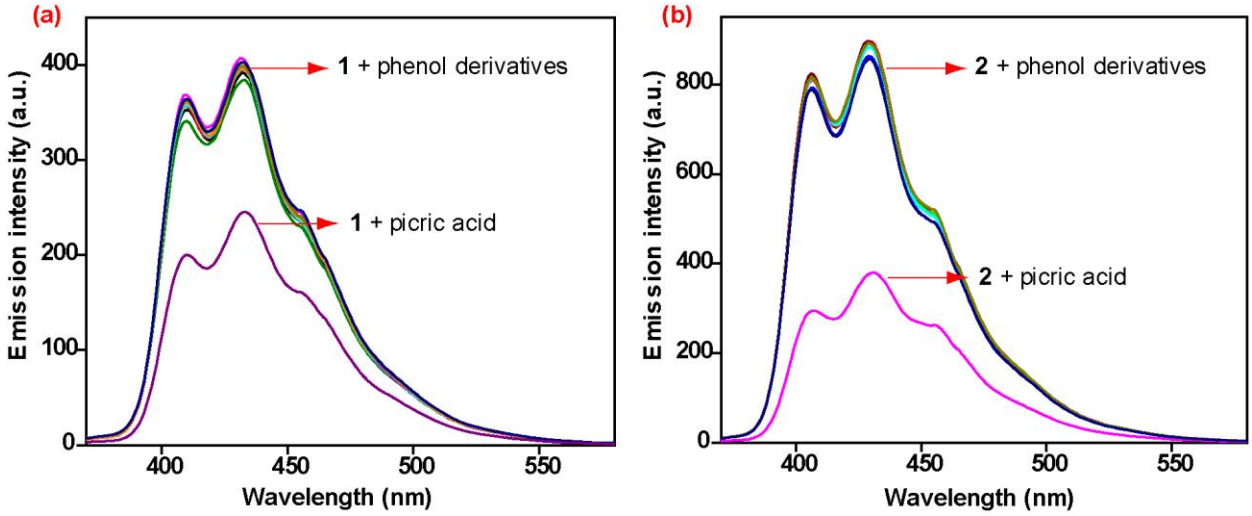

Figure S24. Emission spectra of (a) Pd-macrocycle **1** (1 μM) and (b) Pd-macrocycle **2** (1 μM) in presence of different phenol derivatives (0-20 μM) and picric acid in EtOH. Phenol derivatives used: 4-methoxyphenol, 4-chlorophenol, 2,4-di-tert-butylphenol, 2,6-di-tert-butylphenol, 2,4,6-tri-tert-butylphenol, 2,4,6-trichlorophenol, 2,4,6-tribromophenol, 2,4,6-trimethylphenol and picric acid.

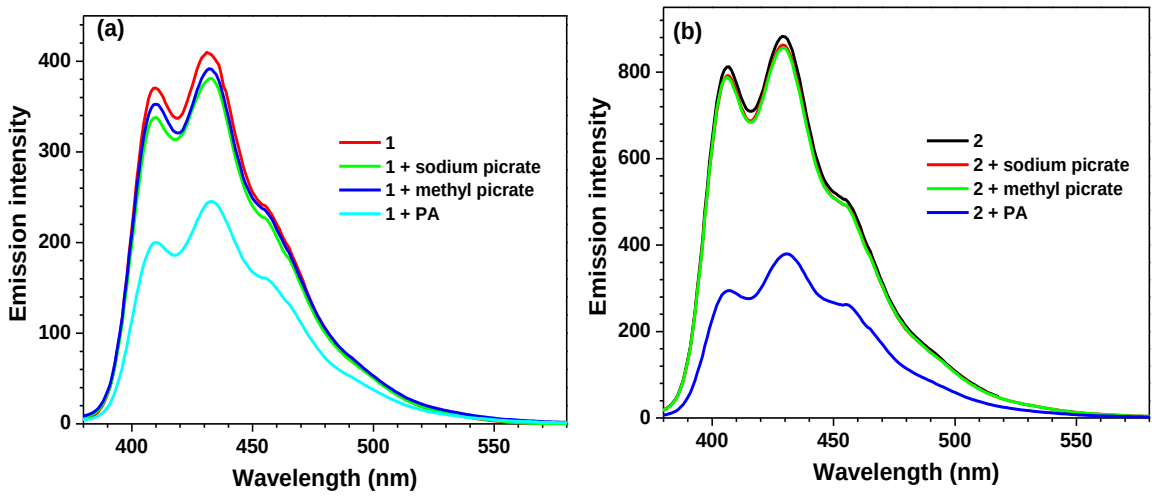

Figure S25. Change in emission intensity of (a) Pd-macrocycle **1** (1 µM) and (b) Pd-macrocycle **2** (1 µM) with sodium picrate, methyl picrate and picric acid (20 µM) in EtOH.

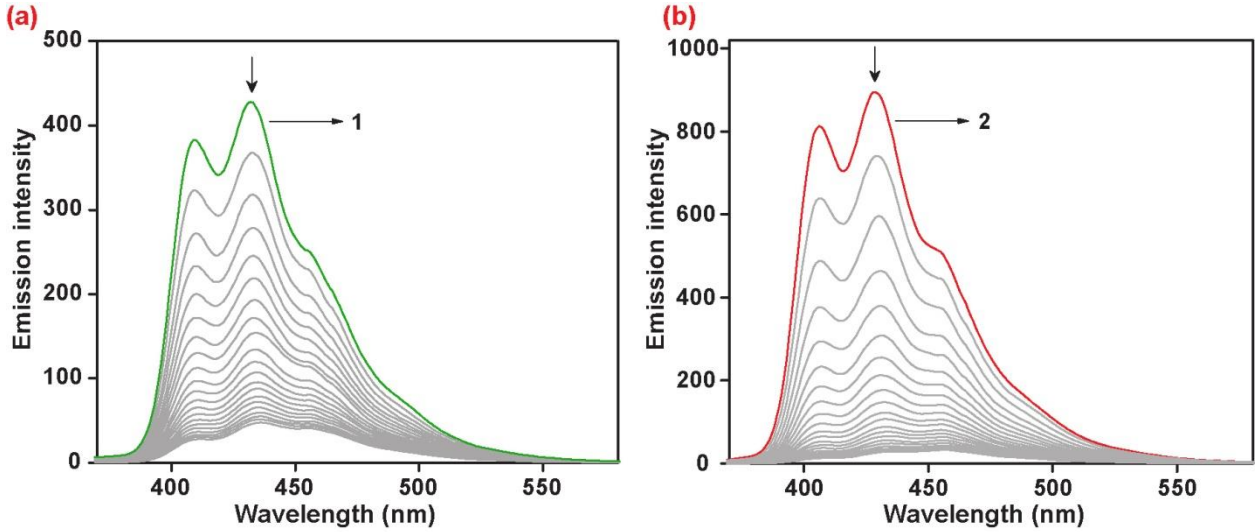

Figure S26. Change in emission intensity of (a) Pd-macrocycle **1** and (b) Pd-macrocycle **2** (1 µM) with quantitative addition of picric acid (0-100 µM) in EtOH.

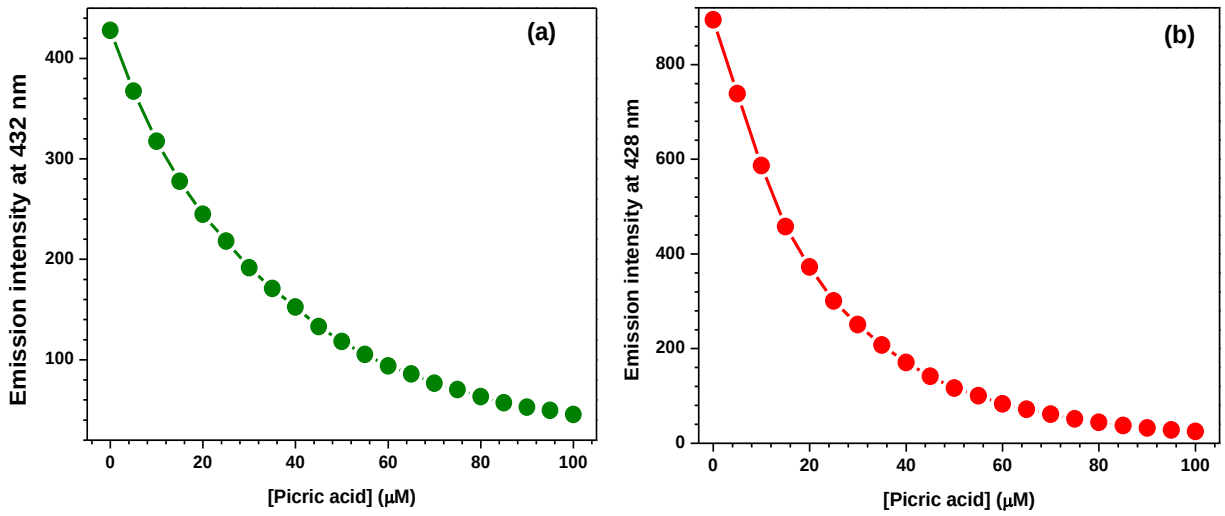

Figure S27. Change in emission intensity of (a) Pd-macrocycle **1** (1 μM) at 432 nm and (b) Pd-macrocycle **2** (1 μM) at 428 nm with picric acid (0-100 μM) in EtOH.

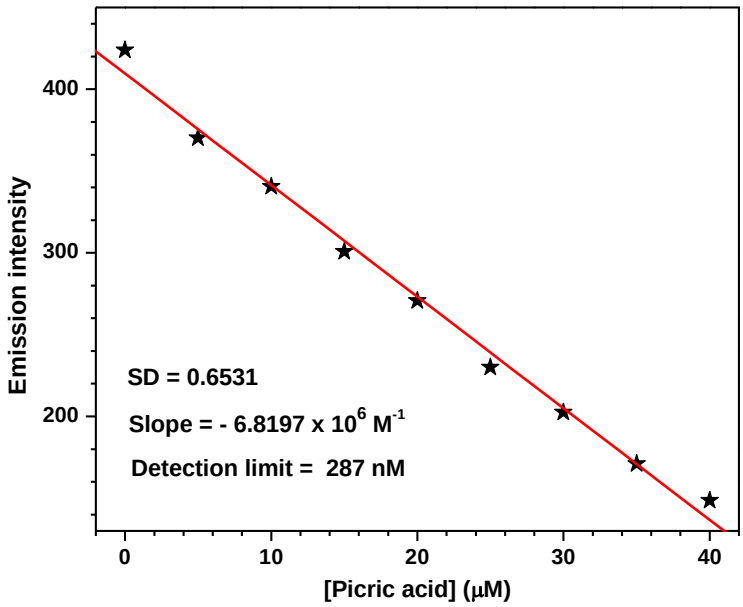

Figure S28. Determination of detection limit of Pd-macrocycle **1** (1 μM) in EtOH towards picric acid (Concentration was linear from 0 – 40 μM).

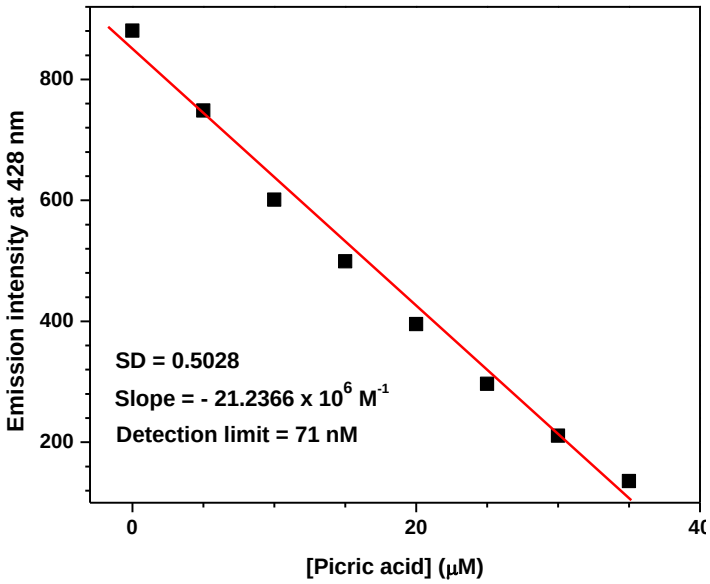

Figure S29. Determination of detection limit of Pd-macrocycle **2** (1 μM) in EtOH towards picric acid (Concentration was linear from 0 – 35 μM).

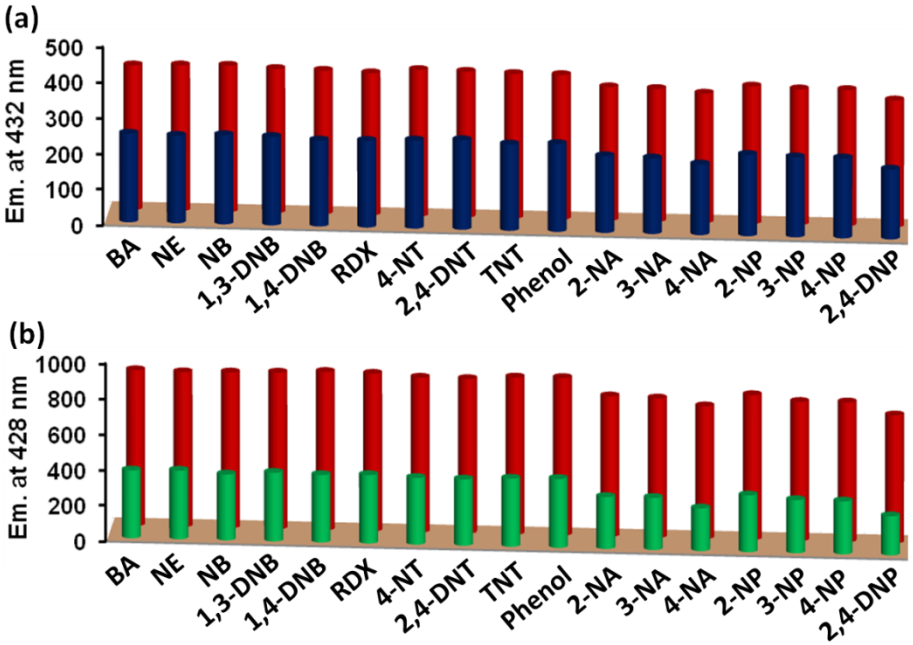

Figure S30. (a) Selectivity of Pd-macrocycle **1** towards PA in presence of other NACs: **1** + NACs (red pillars); and **1** + NACs + PA (blue pillars). (b) Selectivity of Pd-macrocycle **2** towards PA in presence of other NACs: 2 + NACs (red pillars); and 2 + NACs + PA (green pillars).

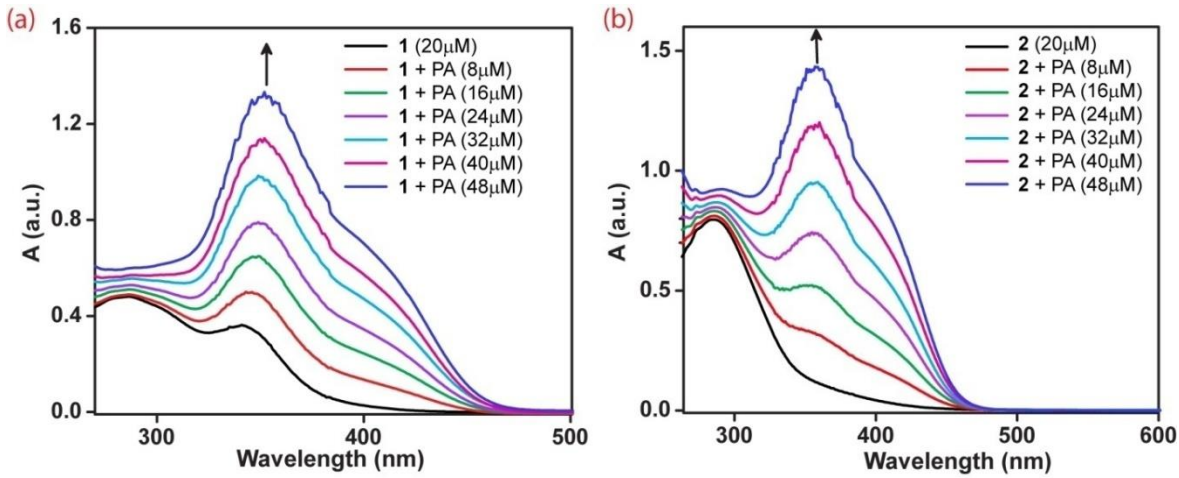

Figure S31. UV-Vis spectral titration of Pd-macrocycles **1** and **2** with PA in EtOH.

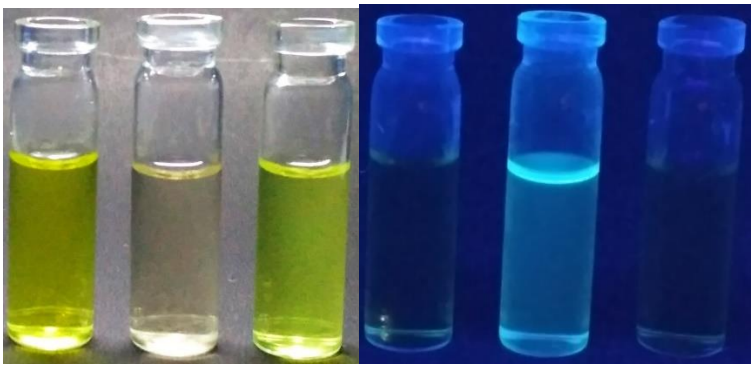

Under visible light **Under ultraviolet light**

Figure S32. Images of response of Pd-macrocycle **2** in EtOH with picric acid (PA) in visible (left) and ultraviolet region (right). In both panels, 1st, 2nd and 3rd tubes respectively represent PA, **2** and **2** + PA.

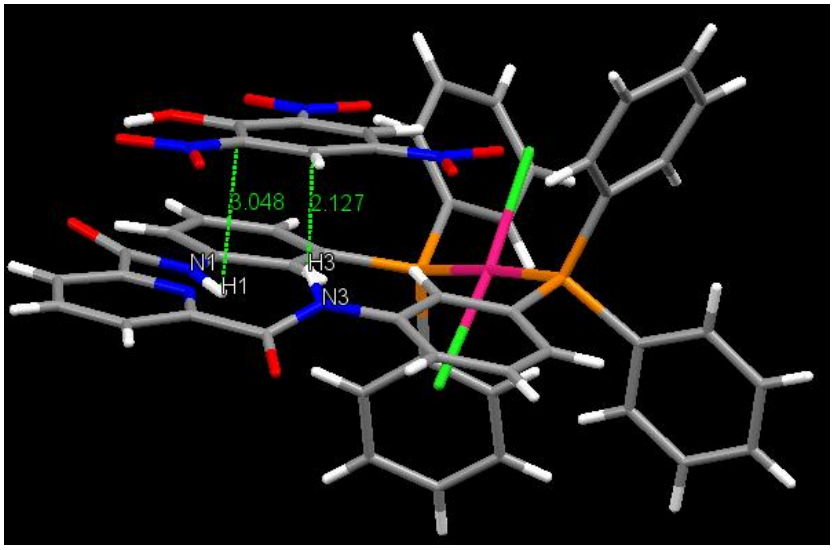

Figure S33. Molecular docking structure of Pd-macrocycle **1** with picric acid (PA).

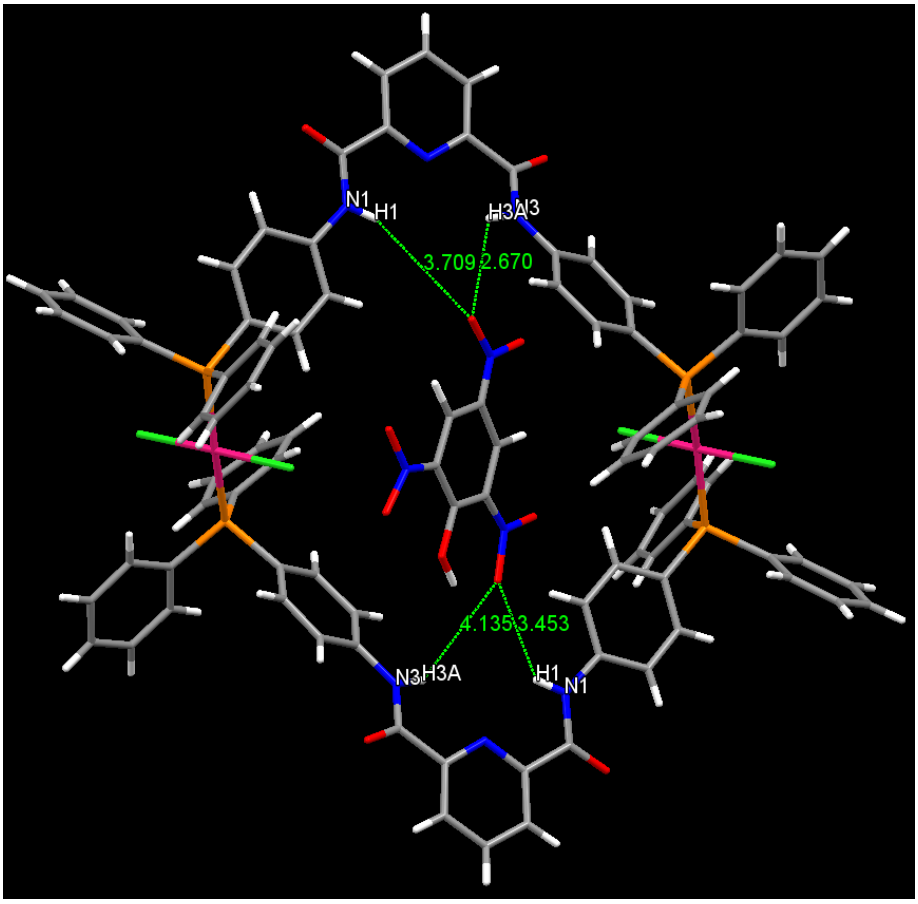

Figure S34. Molecular docking structure of Pd-macrocycle **2** (lower) with picric acid (PA).

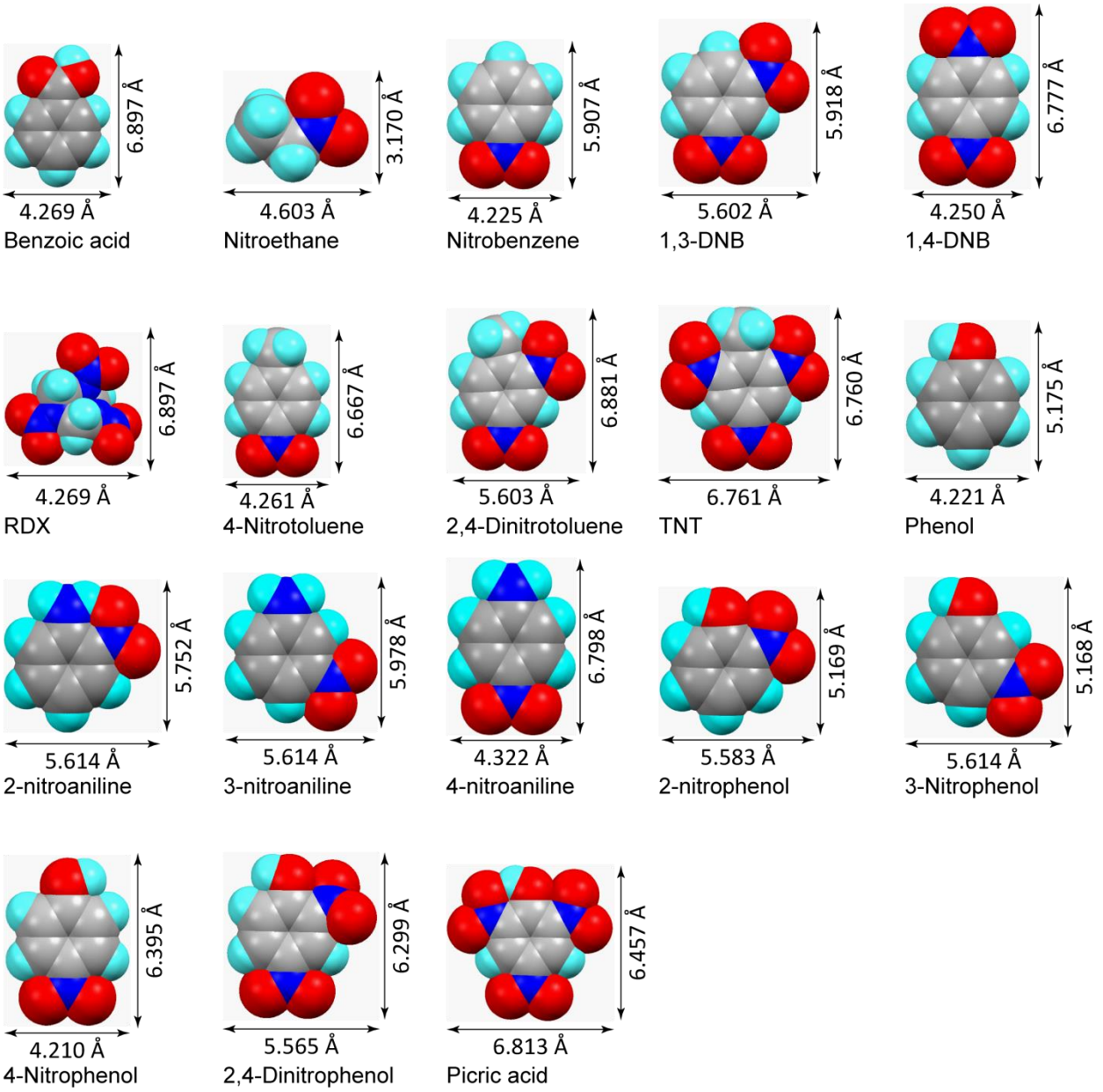

Figure S35. Dimensions of various organic substrates used in the present work. In order to measure the dimension of the mentioned molecule, two suitable atoms were selected and their center-to-center distance was measured by *Chem3D* followed by the addition of their van der Walls radii.

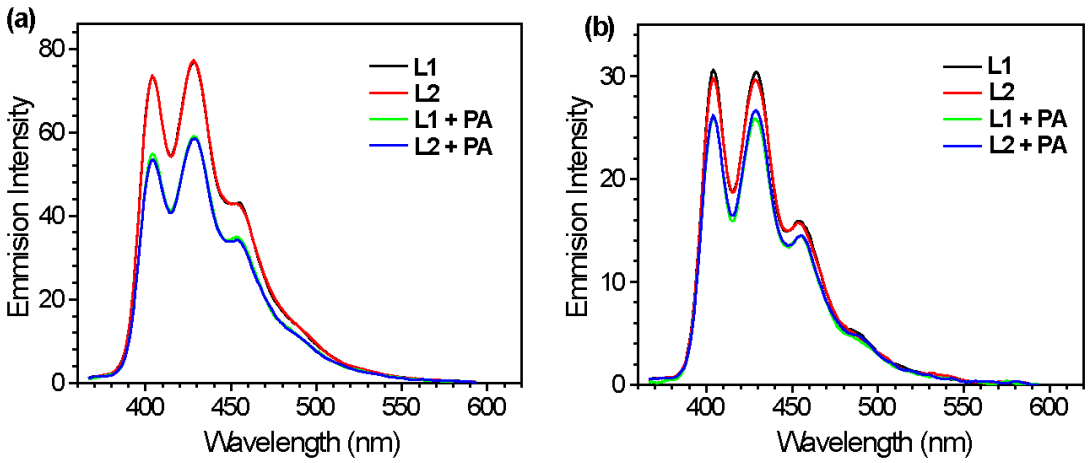

Figure S36. Change in emission of L1 and L2 (1μM) in absence and presence of picric acid (20 μM) (λ_{ex} = 350 nm) (a) in EtOH and (b) in THF.

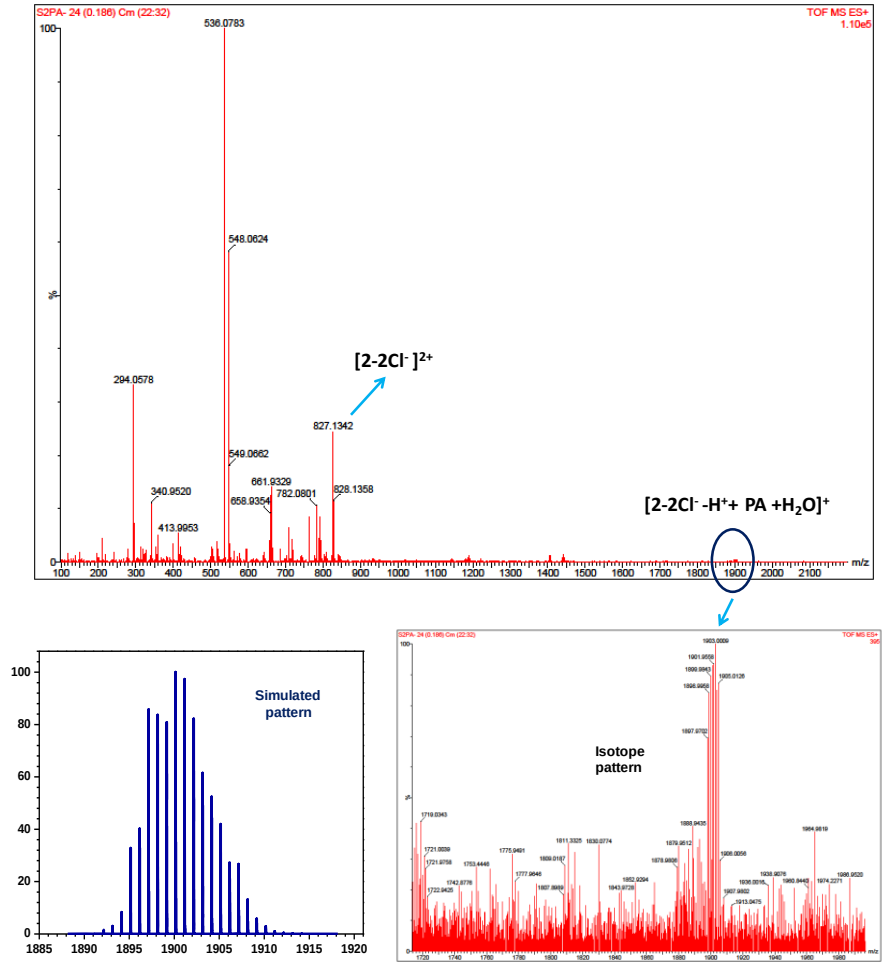

Figure S37. ESI^+-MS spectrum of Pd-macrocycle **2** in presence of PA (recorded in EtOH) with its experimental isotope pattern and the simulated pattern calculated using ChemCalc.

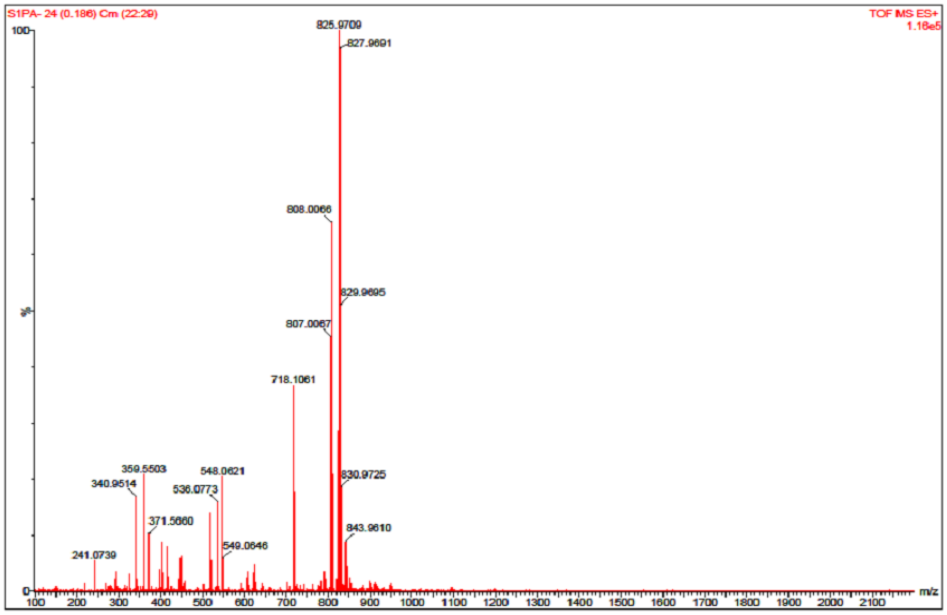

Figure S38. ESI$^+$-MS spectrum of Pd-macrocycle **1** in presence of PA recorded in EtOH.

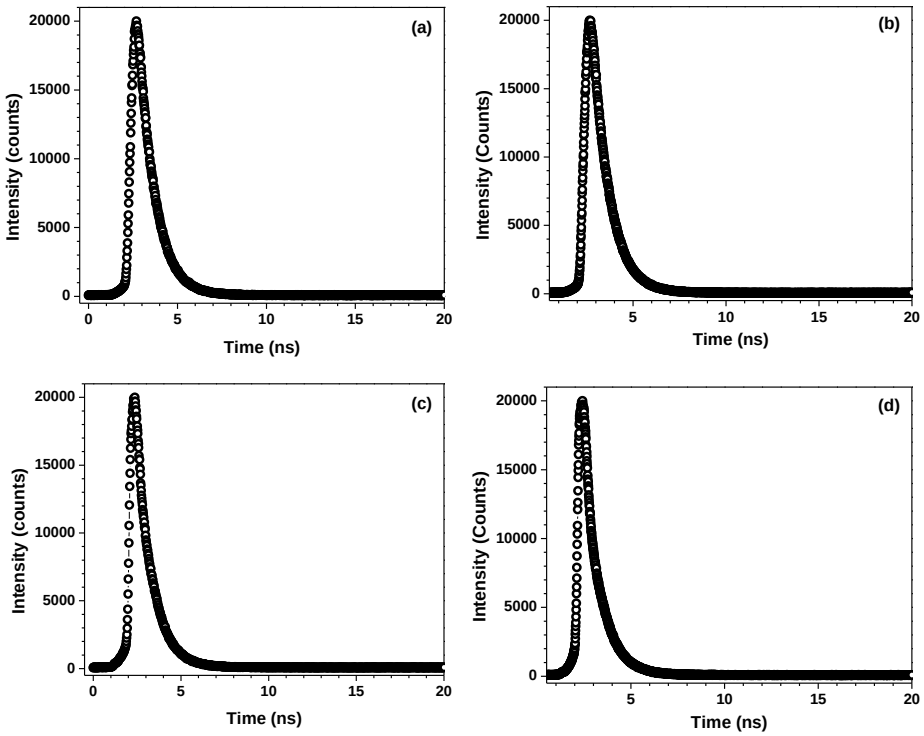

Figure S39. Lifetime profiles for Pd-macrocycles **1** (20 μM) and **2** (20 μM) in absence and in presence of PA (10 equivalents) in ethanol. (λ_{ex} = 406 nm and λ_{em} = 432 nm for **1** and 428 nm for **2**): (a) **1**, (b) **1** + PA, (c) **2**, (d) **2** + PA.

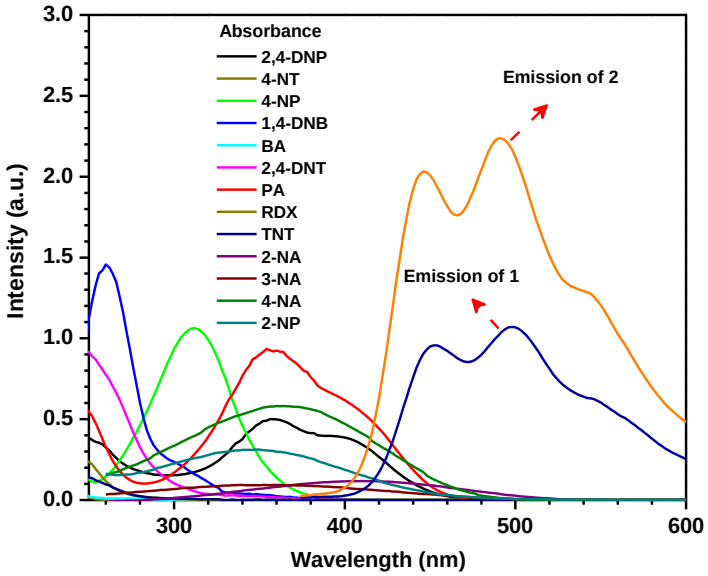

Figure S40. Spectral overlap between the absorption spectra of different NACs and the emission spectra of Pd-macrocycles **1** and **2**.

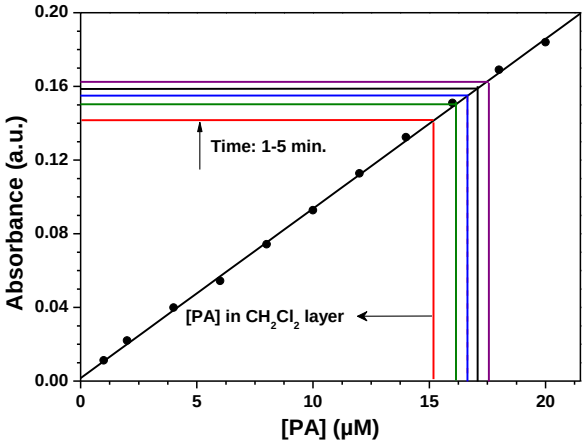

Figure S41. Extraction of PA from an aqueous phase to a CH_2Cl_2 layer mediated by Pd-macrocycle **2**. Five lines shown in different colors exhibit the extraction of PA after 1, 2, 3, 4, and 5 min, respectively. Such lines have been fitted to the calibration plot (black line).

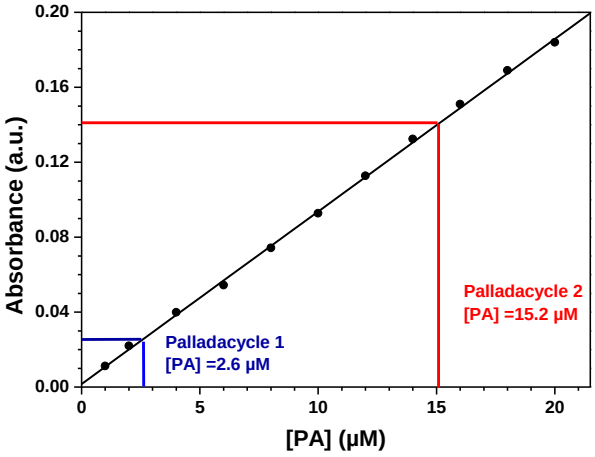

Figure S42. Determination of concentration of PA in CH_2Cl_2 containing Pd-macrocycles **1** and **2** (1μM) after extraction from an aqueous phase. The black line represents the calibration plot.

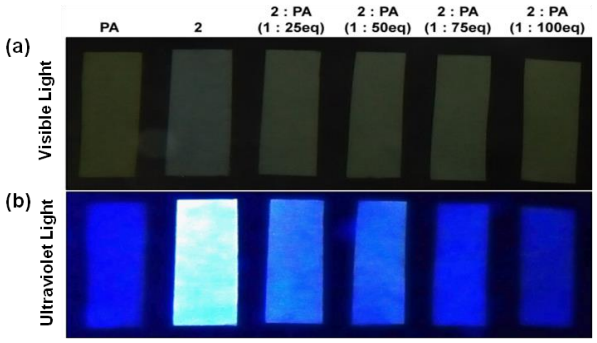

Figure S43. Images of filter paper strips coated with Pd-macrocycle **2** and dipped in an aqueous solution of PA; under the (a) visible and (b) ultraviolet region.

Table S1. Stern-Volmer constants (K_{SV}), detection limits and binding constants (K_b) for Pd-macrocycles **1** and **2** with picric acid (PA).

Species	K_{SV} **(M^{-1})**	**Detection limit (nM)**	K_b **(M^{-1})**
1 + PA	6.73×10^4	287	2.47×10^4
2 + PA	2.61×10^5	71	1.03×10^5

Table S2. Photo-physical characteristics of ligands L1 and L2 and Pd-macrocycles **1** and **2**.

Ligand/ Pd-macrocycle	λ_{ex} **(nm)**	λ_{em} **(nm)**	**Relative quenching (%) by PA**	
			EtOH	**THF**
L1	350	428	23.4	15.6
L2	350	428	24.6	13.1
1	350	432	39.0	26.7
2	350	428	58.1	45.2

Table S3. Lifetime measurement parameters for Pd-macrocycles **1** and **2** in absence and in presence of picric acid (PA) in EtOH.

Pd-macrocycle	τ_{av} **(ns, intensity weighted)**	τ_{av} **(ns, amplitude weighted)**
1	0.3424	0.3424
1 + PA	0.2977	0.2977
2	1.00525	0.88809
2 + PA	0.86928	0.76914

Table S4. Crystallographic data collection and structure refinement parameters for **1** and **2**.

	[**1**]$_2$•CH_3CN	[**2**]$_2$•$(DMF)_4$•$(CH_3OH)_2$
Empirical formula	$C_{88}H_{69}Cl_4N_7O_4P_4Pd_2$	$C_{186}H_{168}Cl_8N_{16}O_{13}P_8Pd_4$
Formula weight	1766.98	3808.51
Temperature	293(2) K	293(2) K
Wavelength	0.71073 Å	0.71073 Å
Crystal system	triclinic	monoclinic
Space group	*P* -1	*P* 21/*c*
a	14.6300(7) Å	12.8662(8) Å
b	17.2897(8) Å	20.0260(9) Å
c	17.3682(8) Å	18.4428(9) Å
α	114.316(4)°	90°
β	99.339(4)°	109.817(7)°
γ	93.502(4)°	90°
Volume	3910.3(3) Å^3	4470.5(4) Å^3
Z	2	1
Density (calculated)	1.501 Mg/m^3	1.408 Mg/m^3
Absorption coefficient	0.736 mm^{-1}	0.651 mm^{-1}
F(000)	1796	1938
Crystal size	0.23 x 0.21 x 0.20 mm^3	0.24 x 0.21 x 0.20 mm^3
Theta range for data collection	2.83 to 24.99°	3.113 to 25.00°
Index ranges	-17 ≤ h ≤ 17, -20 ≤ k ≤ 20, -20 ≤ l ≤ 20	-15 ≤ h ≤ 8, -22 ≤ k ≤ 23, -21 ≤ l ≤ 21
Reflections collected	48785	24408
Independent reflections	13758 [*R*(int) = 0.0753]	7707 [*R*(int) = 0.0874]
Completeness to theta = 25.00°	99.8 %	98.0 %
Absorption correction	Multi-scan	Multi-scan
Max. and min. transmission	0.863 and 0.844	0.878 and 0.855
Refinement method	Full-matrix least-squares on F^2	Full-matrix least-squares on F^2
Data / restraints / parameters	13758 / 1 / 983	7707 / 0 / 542
Goodness-of-fit on F^2	0.991	0.996
Final *R* indices [I>2sigma(I)][a, b]	R_1 = 0.0590, wR_2 = 0.0988	R_1 = 0.0765, wR_2 = 0.1582
R indices (all data)	R_1 = 0.1102, wR_2 = 0.1148	R_1 = 0.1404, wR_2 = 0.1864
Largest diff. peak and hole	0.806 and -0.674 e.Å^{-3}	0.654 and -0.383 e.Å^{-3}
CCDC No.	1582152	1582153

[a] $R = \sum(\|Fo\| - \|Fc\|)/\sum|Fo|$; [b] $wR = \{\sum[w(F_o^2 - F_c^2)^2]/\sum[w(F_o^2)^2]\}^{1/2}$